

# The Mathematics of Linked Optimisation for Water and Nitrogen Use in a Canopy

Thomas N. Buckley, Jeffrey M. Miller and Graham D. Farquhar

---

**Buckley, T.N., Miller, J.M. & Farquhar, G.D.** 2002. The mathematics of linked optimisation for water and nitrogen use in a canopy. *Silva Fennica* 36(3): 639–669.

We develop, and discuss the implementation of, a mathematical framework for inferring optimal patterns of water and nitrogen use. Our analysis is limited to a time scale of one day and a spatial scale consisting of the green canopy of one plant, and we assume that this canopy has fixed quantities of nitrogen and water available for use in photosynthesis. The efficiencies of water and nitrogen use, and the interactions between the two, are strongly affected by physiological and physical properties that can be modeled in different ways. The thrust of this study is therefore to discuss these properties and how they affect the efficiencies of nitrogen and water use, and to demonstrate, qualitatively, the effects of different model assumptions on inferred optimal strategies. Preliminary simulations suggest that the linked optimisation of nitrogen and water use is particularly sensitive to the level of detail in canopy light penetration models (e.g., whether sunlit and shaded fractions are pooled or considered independently), and to assumptions regarding nitrogen and irradiance gradients within leaves (which determine how whole-leaf potential electron transport rate is calculated from leaf nitrogen content and incident irradiance).

**Keywords** nitrogen allocation, NUE, WUE, stomatal conductance, optimality theory.

**Authors' addresses** *Buckley & Farquhar*: Environmental Biology Group, Research School of Biological Sciences, The Australian National University, GPO Box 475, Canberra City, ACT 2601, Australia and Cooperative Research Centre for Greenhouse Accounting, RSBS, ANU; *Miller*: Environmental Biology Group, Research School of Biological Sciences, The Australian National University, GPO Box 475, Canberra City, ACT 2601, Australia

**Fax** +61-02-6125-4919 **E-mail** tom\_buckley@alumni.jmu.edu

**Received** 15 June 2001 **Accepted** 8 July 2002

---

# 1 Introduction

Over the last few decades, our understanding of the ecology of relationships between light, nitrogen, water and carbon within plant canopies has developed considerably. Much of this progress has taken place in the context of an implicit ‘optimality paradigm,’ which recognizes that biological patterns in nature should reflect the tendency of natural selection to preserve strategies that make the most of limited resource supplies. In particular, synthetic theories have emerged to predict basic optimal trends for water use (Cowan 1977, Cowan and Farquhar 1977, Cowan 1982, Cowan 1986, Mäkelä et al. 1996) and nitrogen use (Field 1983, Hirose and Werger 1987, Farquhar 1989, Schieving and Poorter 1999). While extensive testing has generally corroborated the qualitative trends predicted by these single-resource theories (Farquhar et al. 1980a, Field 1983, Hirose and Werger 1987, Werger and Hirose 1991, Schieving et al. 1992, Evans 1993, Berninger et al. 1996, Hari et al. 1999, Koskela et al. 1999, Gonzales-Real and Baille 2000, Hari et al. 2000), these theories have had limited success in replacing the predominantly semi-mechanistic and semi-empirical basis of models for gas exchange at the individual scale and above. For example, the prediction that leaf nitrogen content should scale with irradiance is used to drive canopy models that are otherwise not based explicitly on optimality theory (e.g., Sellers et al. 1992, Amthor et al. 1994, Leuning et al. 1995, Lloyd et al. 1995). Furthermore, the ‘optimal’ profiles used in such models are often quite different from empirically observed profiles, though the assumption is retained because the resulting models can predict gas exchange accurately.

A strong and direct physiological linkage exists between the efficiencies of nitrogen and water use (e.g., Field et al. 1983, Reich et al. 1989, Cordell et al. 1999), and this connection may be responsible for the limited success of theories that deal with only one of these two resources. By identifying ‘linked optima,’ that is, by simultaneously optimizing both resources – as a plant in nature must do when faced with limited supplies of water and nitrogen – it may be possible to begin to make effective, testable predictions of

whole-plant gas exchange strictly on the basis of optimality theory. However, the rigorous linked optimality criteria require calculation of the sensitivity of spatially and temporally integrated gas exchange patterns to changes in resource allocation strategies, and these sensitivities can not be calculated analytically.

The goals of the present work were to provide a complete conceptual and mathematical framework for the simultaneous optimization of nitrogen and water use in a canopy (including derivations of key equations that are too detailed and esoteric to present in more applied work), to identify important features for inclusion in a simulation model that will perform this optimization, to demonstrate the effects of these features, and to raise salient questions for more detailed analysis. We present the abstract mathematical solution for water and nitrogen use optimisation in a single plant in Section 2, and attempt to resolve conceptual difficulties in its interpretation and potential ambiguities in its implementation. In Section 3 we discuss physiological and physical considerations that can strongly affect the relationships between assimilation rate and water and nitrogen use, and which can, therefore, also change the optimal nitrogen profiles that one would infer from a simulation model. We demonstrate these effects graphically by manipulating a leaf gas exchange model (presented in the Appendix) and by inferring optimal nitrogen profiles from a detailed canopy simulation model (based on the models presented by Leuning et al. (1995) and de Pury and Farquhar (1997), but not presented in detail here). Finally, in Section 4, we summarize the analyses of Sections 2 and 3, suggest applications of the mathematical framework developed in this paper, and offer some thoughts on the role of optimality theory in plant ecophysiology. In the Appendix, we apply the abstract optimal solution (from Section 2) to a general model of leaf gas exchange, to develop mathematical expressions that can be used in detailed simulation models of canopy gas exchange. In an accompanying paper (Farquhar et al. 2002), we apply the abstract solution to a more simplified gas exchange model (which excludes self-shading and temperature effects) to evaluate general ecological implications of linked optimal water and nitrogen use.

## 2 Abstract Mathematical Solution for Nitrogen and Water Co-Optimisation

### 2.1 Statement of the Problem and Its General Solution

We will begin by arbitrarily defining the term *optimal*, with regard to resource use strategies, as describing a strategy that maximizes the ratio of daily net CO<sub>2</sub> assimilation to the available quantity of resource. Many other definitions are possible, including reproductive success (the ultimate goal from a Darwinian perspective) and assimilation averaged over a longer time period. However, reduced carbon can be used for nearly any purpose (e.g., building seeds to reproduce, leaves to compete for light, or protective structures to ward off predators), and a single day is a convenient temporal context that subsumes much of the predictable variation in environmental factors that an individual plant faces. Therefore, we believe this definition of ‘optimal’ represents an appropriate compromise between generality and relevance, and proceed with no further discussion of the term. Givnish (1986) has discussed this issue in depth.

Our problem is formally stated as follows: Suppose a plant has a finite daily water supply,  $E_t$ , and a finite amount of functional nitrogen in its leaves,  $N_t$ . (These terms represent, respectively, the transpiration rate per unit leaf area,  $E$ , integrated over all leaves in the plant and over one day, and the leaf nitrogen content per unit leaf area,  $N$ , integrated over all leaves in the plant). The goal is to maximize the plant’s net carbon gain in a single day,  $A_t$  (the integral of leaf net CO<sub>2</sub> assimilation rate,  $A$ , over a day and over all leaves in the plant). Therefore, we wish to know how the control variables, which are stomatal conductance ( $g_{sc}$ ) and leaf nitrogen content ( $N$ ), should vary among leaves (and, for  $g_{sc}$ , over the course of the day) in order to maximize  $A_t$ . Formally, the solution to this problem is the set of functions,  $g_{sc}(t, L)$  and  $N(L)$ , that maximizes  $A_t$  in the following expression:

$$A_t[g_{sc}(t, L), N(L)] \equiv \int_{day} \int_{L_t}^0 A(g_{sc}(t, L), N(L)) dL dt \tag{1}$$

(In Eq 1,  $L$  is cumulative leaf area index, which ordinates the ‘position’ of a leaf relative to the uppermost leaf layer,  $L_t$  is total canopy leaf area index, and  $t$  is time. Note, however, that the subscript ‘ $t$ ’ in  $A_t$ ,  $E_t$ , and  $N_t$  denotes *total* rather than time.) The calculus of variations can be used to obtain the following solution (e.g., Wan 1995, p. 461–463):

$$\lambda \Lambda A(g_{sc}) \equiv \Lambda E(g_{sc}) \tag{2}$$

$$\text{where } \Lambda \equiv \left( \frac{\partial}{\partial g_{sc}} - \frac{\partial}{\partial L} \frac{\partial}{\partial (g_{sc}/\partial L)} + \frac{\partial}{\partial t} \frac{\partial}{\partial (g_{sc}/\partial t)} \right)$$

$$\eta H \bar{A}(N) \Big|_L \equiv H N \tag{3}$$

$$\text{where } H \equiv \left( \frac{\partial}{\partial N} - \frac{\partial}{\partial L} \frac{\partial}{\partial (dN/dL)} \right)$$

In Eq 3,  $\bar{A} \Big|_L$  is the mean of  $A$  over a single day in a layer  $L$ :

$$\bar{A} \Big|_L \equiv \int_{day} A(N, L) dt \Big/ \int_{day} dt \tag{4}$$

(Note that Eqs 3 and 4 could also be expressed in terms of the *total* of  $A$  over the day in the layer  $L$ , in which case the numerical value of  $\eta$  would simply differ by a factor equal to the daylength.) The Lagrange multiplier  $\lambda$  is a constant over the domain of  $E$  and  $g_{sc}$  (which is time and cumulative leaf area index), and the multiplier  $\eta$  is a constant over the domain of  $N$  (which is cumulative leaf area index). Because  $A$ ,  $E$  and  $N$  are state functions with respect to  $g_{sc}$  and  $N$  (in other words,  $A$ ,  $E$  and  $N$  can be calculated knowing the values of  $g_{sc}$  and  $N$  *only* at the local point in time and space, and without knowing how  $g_{sc}$  and  $N$  vary around that point), their derivatives with respect to  $\partial g_{sc}/\partial L$ ,  $\partial g_{sc}/\partial t$ , and  $\partial N/\partial L$  are zero. Therefore, the operators  $\Lambda$  and  $H$  degenerate to  $\partial/\partial E$  and  $\partial/\partial N$ , respectively, and Eqs 2 and 3 reduce to Eqs 5 and 6, respectively:

$$\frac{\partial A}{\partial E} \stackrel{opt}{=} \frac{1}{\lambda} \tag{5}$$

$$\frac{\partial \bar{A}}{\partial N} \stackrel{opt}{=} \frac{1}{\eta} \tag{6}$$

The equalities in Eqs 5 and 6 are expressed with the distinct notation of ‘optimal identities,’

because they represent relations that hold at, and only at, the optimum. In general, the quantities  $\partial A/\partial E$  and  $\partial A/\partial N$  can differ among leaves, but in an optimal plant, they are everywhere equal to  $1/\lambda$  and  $1/\eta$ , respectively. This is discussed in Section 2.4.

## 2.2 Domains of Differentiation

Eqs 5 and 6 are strictly ambiguous, because partial derivatives can be used to express relative changes in two variables when *any arbitrary subset* of the other variables in the system remain constant. We must therefore be careful to identify which variables can change, and which cannot, as  $E$  and  $N$  vary in Eqs 5 and 6.

These derivatives express gradients in  $A$  along domains of ‘candidate’ values of  $E$  (or more precisely,  $g_{sc}$ ) and of  $N$ . Neither Eqs 5 nor 6 allow any externally imposed environmental variables to vary. (If we believe that leaf gas exchange can significantly affect the atmospheric conditions within the canopy, this assumption must be revised; however, we proceed on the assumption that the ambient humidity,  $\text{CO}_2$  partial pressure, air temperature, wind speed, incident irradiance, and absorbed radiation are independent of leaf gas exchange *per se*.) In Eq 5, we can safely assume that  $N$  will not differ among candidate values of  $g_{sc}$  at the same point in  $(t, L)$  space; however, the leaf temperature, intercellular  $\text{CO}_2$  partial pressure, and evaporative gradient may change with  $E$ , and therefore must be allowed to vary among candidate values of  $g_{sc}$ . For Eq 6, the ‘variables’ whose constancy or variability we must evaluate are in fact functions of time over a single day, because the optimization domain of  $N(L)$  and  $\bar{A}$  subsumes a whole day. In this case, the daily timecourse of stomatal conductance  $g_{sc}$  (and thus transpiration rate,  $E$ , and all variables that can change with  $E$ ) may respond to changes in photosynthetic capacity among candidate  $N$  values.

This distinction can be confusing, because it is reasonable to ask, When would such variation of  $g_{sc}$  with  $N$  actually be observed in an optimal canopy? There is no clear answer to that question, because it involves an open physiological problem: *how* do these allocation controls oper-

ate in real plants experiencing changing conditions? Perhaps  $g_{sc}$  would be observed to vary with  $N$  as nitrogen is reallocated among leaves in response to an externally imposed change in the light environment (for example, if a forest gap opened up nearby due to logging needed to supply optimality theorists with paper on which to print their many equations). We claim no novel insight to answer this question. Our mathematics do not describe the *mechanisms* or physiological processes by which plants optimise resource allocation; rather, we describe properties of gas exchange in plants that have optimised the use of finite resources (by unknown means that do not concern us). Investigators can use the expressions that we provide to infer optimal resource use strategies from abstract models, and to evaluate the proximity of observed states of real plants to those theoretical optima. It is therefore critical to identify precisely the equations that characterize the optima.

These equations specify that the marginal gain in net assimilation rate associated with an increase in either  $N$  or  $E$  should be uniform over all *possible* domains. If we assume that the smallest time domain on which  $N$  can change is one day, then the marginal gain of assimilation rate with  $N$  must allow for the potential response of stomata to the changes in photosynthetic capacity resulting from a change in  $N$ . On the other hand, the marginal gain of assimilation with  $E$  occurs on a time domain vastly shorter than the rate at which  $N$  can respond to anything, so  $N$  must be considered a constant when calculating the marginal gain of  $A$  with  $E$ .

To summarize, both Eqs 5 and 6 assume that external environmental conditions are independent (so their timecourses are constant); Eq 5 allows all physiological variables except  $N$  to vary as  $E$  varies at a single point in  $(t, L)$  space; and Eq 6 allows the timecourses of all physiological variables to vary as  $N$  varies at a single point in  $(L)$  space. We will denote these refinements by enclosing the partial derivatives in parentheses and adding subscripts with the names of the variables to be considered constants:

$$\left(\frac{\partial A}{\partial E}\right)_{N,env} \stackrel{opt}{=} \frac{1}{\lambda} \quad (7)$$

$$\left(\frac{\partial \bar{A}}{\partial N}\right)_{env} \stackrel{opt}{=} \frac{1}{\eta} \tag{8}$$

In these equations, the subscript ‘env’ refers to all externally imposed environmental variables that are not directly affected by transpiration or assimilation.

### 2.3 Domains of Differentiation: Reprise

Note that the ‘optimality criteria’ in Eqs 7 and 8 are not explicitly linked, in the sense that optimal water use is defined by Eq 7 alone, and optimal nitrogen use is defined by Eq 8 alone. In the preceding section we argued, on the physiological basis that nitrogen and water use ‘decisions’ are made on very different time scales, that the optimally invariant derivative of  $A$  with respect to  $N$  must allow conductance (and therefore  $E$ ) to vary. However, the interpretation and analytical calculation of  $\eta$  is complicated greatly by the implicit freedom of  $E$  (see Eqs A55 to A60 in the Appendix). It turns out that these complications can be ignored when water and nitrogen are being co-optimized. To develop this simplification, observe that daily assimilation can be expressed and differentiated as a bivariate function of  $E$  and  $N$ , i.e.,  $A = A(N, E)$ :

$$\begin{aligned} \frac{d\bar{A}}{dN} &= \frac{d}{dN} \left[ \frac{\int_{day} A(N, E(t)) dt}{\int_{day} dt} \right] = \frac{1}{t_{dl}} \int_{day} \frac{dA}{dN} dt \\ &= \frac{1}{t_{dl}} \int_{day} \left[ \left(\frac{\partial A}{\partial N}\right)_E + \left(\frac{\partial A}{\partial E}\right)_N \frac{dE}{dN} \right] dt \tag{9} \\ \Rightarrow \frac{1}{\eta} &= \frac{1}{t_{dl}} \left( \int_{day} \left(\frac{\partial A}{\partial N}\right)_E dt + \int_{day} \left(\frac{\partial A}{\partial E}\right)_N \frac{dE}{dN} dt \right) \end{aligned}$$

(The integral of time in the first expression has been replaced with  $t_{dl}$ , the daylength.) The terms in the integrand of Eq 9 may vary with position in the canopy ( $L$ ), because nothing in the preceding derivation constrains them to invariance among layers. Suppose a small amount of nitrogen, say

$\delta N$ , is moved from one layer ( $L = L_1$ ) to another layer ( $L = L_2$ ) in a canopy where nitrogen and water are used optimally. Using subscripts to denote layers,  $\delta N_1 = -\delta N_2$ . This leads to

$$\delta N_1 \left(\frac{1}{\eta}\right)_1 = -\delta N_2 \left(\frac{1}{\eta}\right)_2 \tag{10}$$

Applying Eq 10 to 9, rearranging, eliminating  $t_{dl}$ , and using  $\delta N \cdot dE/dN = \delta E$ , we have

$$\begin{aligned} \delta N_1 \left( \int_{day} \left(\frac{\partial A}{\partial N}\right)_{E,1} dt - \int_{day} \left(\frac{\partial A}{\partial N}\right)_{E,2} dt \right) \\ = \left( \int_{day} \left(\frac{\partial A}{\partial E}\right)_{N,2} \delta E_2 dt + \int_{day} \left(\frac{\partial A}{\partial E}\right)_{N,1} \delta E_1 dt \right) \end{aligned} \tag{11}$$

Because water use is assumed optimal,  $\partial A/\partial E$  is constant (and equal to  $1/\lambda$ ) and can be pulled out of the integrals on the right-hand side of Eq 11. However, the integrals that then remain,  $\int \delta E_2 dt$  and  $\int \delta E_1 dt$ , must be equal and opposite to satisfy the constraint on daily water use ( $E_t$ ). This causes the right side of Eq 11 to vanish, forcing the left side equal to zero. This has two major implications:

$$\int_{day} \left(\frac{\partial A}{\partial N}\right)_{E,1} dt = \int_{day} \left(\frac{\partial A}{\partial N}\right)_{E,2} dt \tag{12}$$

$$\int_{day} \left(\frac{dE}{dN}\right)_1 dt = \int_{day} \left(\frac{dE}{dN}\right)_2 dt \tag{13}$$

(The second result is obtained by removing  $1/\lambda$  from the integrals on the right side of Eq 9, and decomposing  $\delta E$  back into  $\delta N \cdot dE/dN$ .) Since layers 1 and 2 are arbitrary, the equalities in Eqs 12 and 13 specify an invariance among all canopy layers. Bringing  $1/t_{dl}$  back into the equations and expressing the integrals as daily average values (indicated by overbars),

$$\overline{\left(\frac{\partial A}{\partial N}\right)_E} \stackrel{opt}{=} \frac{1}{v} \tag{14}$$

$$\overline{\frac{dE}{dN}} \stackrel{opt}{=} \frac{1}{\zeta} \tag{15}$$

where  $\nu$  and  $\zeta$  ( $\nu$  and  $\zeta$ ) are constants among layers in a canopy with optimal nitrogen use, in the same sense that  $\eta$  is a constant. Eq 15 is a very important result, because it formally expresses the intuitive notion that stomatal conductance should track photosynthetic capacity (Wong et al. 1979). Informally, this equation might be translated to say, ‘If a leaf somehow acquires a bit more nitrogen, then stomatal conductance should also increase a bit, so that the increase in leaf nitrogen content is matched by an increase in transpiration rate.’ Alternately, ‘if nitrogen is moved from one leaf to another, water [i.e., transpiration rate] should follow.’ Furthermore, Eq 15 shows that transpiration rate, rather than conductance *per se*, should track leaf nitrogen content, rather than photosynthetic capacity *per se*.

Eqs 14 and 15 form a corollary of Eq 8 that applies when total canopy transpiration rate is constant and water use is optimal. The condition in Eq 14 – invariance of  $\nu$  among canopy layers – may be used interchangeably with invariance of  $\eta$  as a criterion for optimal nitrogen use in such a canopy. In summary, we have shown that the general criterion for optimal nitrogen use is invariance (among canopy layers) in  $1/\eta$ , the total derivative of  $A$  with respect to  $N$  (Eq 8). When a finite water supply is also being used optimally, invariance in  $1/\nu$ , the partial derivative of  $A$  with respect to  $N$  at constant  $E$ , suffices to guarantee optimal nitrogen use.

## 2.4 What Exactly Do Lambda and Eta ( $\lambda$ and $\eta$ ) Mean?

This subsection presents an informal synopsis of the problem and its solution (which were presented formally and mathematically in Section 2.1), with the hope of clarifying its solution. The problem is this: *An individual plant has a finite, fixed supply of each resource.* The water supply is symbolized by  $E_t$  (meaning total transpiration rate; note that this subscript  $t$  denotes *total*, rather than *time*) and the nitrogen supply by  $N_t$  (total nitrogen content). The solution is this: *if a small additional amount of either resource becomes available, it should produce the same increase in carbon gain wherever it is invested.* The small increase in transpiration rate that causes a given

increase in assimilation rate (the ‘marginal cost’ of carbon in units of water) is represented by the Greek symbol lambda ( $\lambda$ ), and the marginal cost of carbon in units of nitrogen is denoted by eta ( $\eta$ ).

Three key points help in interpreting these quantities. First, the marginal gains ( $\partial A/\partial E$  and  $\partial A/\partial N$ ) must be distinguished from *their numerical values in an optimal plant* ( $\lambda$  and  $\eta$ ). The marginal gains can be calculated for any leaf in any plant, whether that plant has optimal resource use strategies or not. On the other hand,  $\lambda$  and  $\nu$  are abstract constructs that can not be measured; they can only be inferred, mathematically, from a model of plant functioning. To clarify this distinction, Eqs 7 and 8 use a special notation – the ‘identity’ symbol,  $\equiv$ , with the letters ‘*opt*’ written over the symbol – to represent a definite equality that holds at (and only at) the optimum, and which therefore defines the optimum. This notation may be translated in English to “... is, in an optimal plant, equal to ...”.

Second,  $\lambda$  is not a unique function of  $E_t$ , nor is  $\eta$  a unique function of  $N_t$ . Both  $\lambda$  and  $\eta$  are complex functions of  $E_t$ ,  $N_t$ , and the surrounding environmental conditions. It is quite easy to become confused about whether  $\lambda$  and  $\eta$  are constants or variables, so we wish to emphasize the following point:  $\lambda$  and  $\eta$  are constant *within* a single plant that has fixed supplies of water and nitrogen and that uses these supplies optimally, but  $\lambda$  and  $\eta$  may vary *among* plants, and they may vary for a single plant on time scales long enough that  $E_t$  and  $N_t$  can change.

Third, if we imagine the plant comparing ‘candidate’ resource-use strategies in order to find the best one, all of the candidates have the same values of  $E_t$  and  $N_t$ , but not necessarily (and not generally) the same values of  $\lambda$  and  $\eta$ . In fact, only one of these candidate strategies (the optimal one) can even be described by a unique pair of values for  $\lambda$  and  $\eta$ , because, by definition, one or both marginal gains varies within the plant in all suboptimal strategies.

### 3 Gas-Exchange Model Features that Can Affect Calculated Optimal Strategies

#### 3.1 Overview: Interactions between the Economies of Water and Nitrogen Use

How are the optimization of canopy nitrogen and water use linked, that is, why do we suppose that these two processes are fundamentally interdependent? First we must carefully define the scope of this question: we are not asking questions about the efficiency of resource acquisition or transport, nor of assimilate partitioning. Those issues require treatment of long-term feedbacks between the allocation of what we may call 'primary resources' (water and nitrogen in this case) and allocation of the secondary resource (fixed carbon) that is procured by the allocation of primary resources. We wish to determine how fixed supplies of nitrogen and water should be used by the leaves of an individual plant (one 'canopy'), where the goal is to maximize the quantity of carbon gained by using these resources. The question is implicitly confined to a time scale on which the resource supplies do not change. For example, the effects of periodic drought or changing litter quality are categorically excluded from this analysis.

The 'linkage' question then becomes, How do nitrogen use and water use interact in leaves? To conceptualize the mutual influences between nitrogen and water, it is helpful to think of them as currencies used to purchase two commodities (light and CO<sub>2</sub>) which are then combined in the leaf to yield a product (carbohydrate). However, there is an interesting twist to this analogy. The 'price' of one of the commodities (CO<sub>2</sub>) decreases as the rate of production increases, making the two currencies somewhat interchangeable: by investing more nitrogen in photosynthetic machinery, the leaf can decrease the cost of carbon in units of water (mechanistically, greater photosynthetic demand draws down  $c_i$ , the CO<sub>2</sub> partial pressure within the leaf; this increases the diffusion gradient, requiring lower stomatal conductance, and therefore less water use, for a

given photosynthetic rate). Conversely, by investing more water, i.e., by opening stomata, the leaf can decrease the cost of carbon in units of nitrogen (higher stomatal conductance increases  $c_i$ , requiring less nitrogen to sustain a given photosynthetic rate). This means that a plant can, to some extent, substitute the more abundant of these two resources for the less abundant one. This leads to the interesting hypothesis, borne out by some evidence (Field et al. 1983, Reich et al. 1989, Cordell et al. 1999) that nitrogen use efficiency (NUE, the ratio of CO<sub>2</sub> assimilation rate,  $A$ , to nitrogen content,  $N$ , or nitrogen flux,  $j_N$ ) and water use efficiency (WUE, the ratio of  $A$  to transpiration rate,  $E$ ) should be inversely related when the comparison is performed among, rather than within, individual plants.

These nitrogen-water interactions are implicit in accepted small-scale biophysical and biochemical models of leaf gas exchange. Carbon dioxide demand is controlled by nitrogen via investment in photosynthetic enzymes (Evans 1983, Field and Mooney 1986), CO<sub>2</sub> supply is controlled by water via stomatal conductance (Farquhar and Sharkey 1982), and the two controls interact via  $c_i$ . What remains to be determined, however, is the role of nitrogen-water interactions *per se* – particularly substitution – in the *optimal* use of these two resources. Because this optimality problem is defined by finite supplies of both resources at the whole-plant scale, nitrogen-water interactions and substitution may complicate attempts to extend the optimal control of gas exchange to whole plants (Field 1991).

In this section, we discuss several major features of gas exchange modeling as they relate to the efficiency of nitrogen and water use. Our goal is to identify features that can have a large influence on predicted optimal strategies for nitrogen and water use.

#### 3.2 Complex Light Environment

The allocation of nitrogen in proportion to available light (photosynthetic photon flux density, irradiance) is a rather hazy problem, because, whereas the irradiance incident on a leaf can change on arbitrarily short time scales (e.g., Hari et al. 1984, Smolander 1984, Korpilahti 1988,

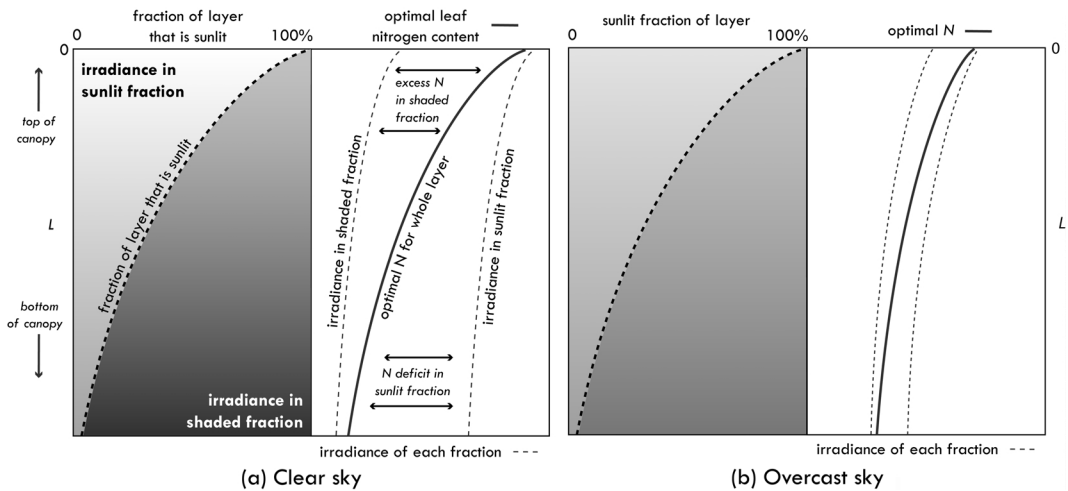


**Fig. 1.** Diagrammatic representation of the sunlit/shaded dichotomy and its qualitative effect on optimal nitrogen allocation. Near the top of the canopy, most leaf area is sunlit, but the opposite is true deeper in the canopy (dashed line in the panel at far left). Because the optimal leaf nitrogen content tracks incident irradiance (to some degree), the optimal *N* is ‘pulled’ toward the sunlit irradiance at the top of the canopy, but to the shaded irradiance near the bottom of the canopy. As a result, deep-canopy leaves are relatively more nitrogen-limited, when sunlit, than top-canopy leaves, whereas top-canopy leaves have an excess of nitrogen during the brief periods that they are shaded. This effect is larger in sunny conditions (a) than it is in overcast conditions (b), because the difference between the sunlit and shaded irradiances is much smaller in overcast conditions.

Pearcy 1990), leaf nitrogen content probably does not change on time scales shorter than a single day. Light intensity at the top of a canopy varies through a day as the Earth rotates. In addition, upper canopy leaves may intercept beam light that would otherwise reach lower leaves, and as the sun tracks across the sky and shifts the position of these shadows and their complementary sunflecks, the canopy creates a temporal distribution of irradiance that is non-uniform on very short time scales for any given leaf. There will generally be at least two modes in this distribution (one for beam light, and one for diffuse and scattered light), and in reality many distinct modes will usually exist (including many penumbra, caused by the sun’s angular width, by diffraction, and by interference among other penumbra; Oker-Blom (1986)); for simplicity we will compare unimodal and bimodal distributions, because they represent extreme cases.

The optimal leaf nitrogen content (*N*) for a bimodal irradiance distribution will not generally appear optimal if evaluated at either of the two

modal irradiances, because the optimal value represents a compromise between the two extremes. In particular, if the leaf were always at the ‘sunlit’ irradiance, the optimal *N* would be higher than for a leaf that spends time at both irradiances (de Pury and Farquhar 1997). This is illustrated diagrammatically in Fig. 1, which shows that leaves near the bottom of the canopy (where the leaves spend very little time at the higher, sunlit irradiance) have a ‘nitrogen deficit’ while they are sunlit, whereas leaves near the top of the canopy (which spend very little time at the ‘shaded’ irradiance) have an excess of nitrogen while they are shaded. Ironically, this results in an optimal nitrogen distribution wherein upper canopy leaves are more light-limited than lower canopy leaves when both are sunlit, because sunlit lower-canopy leaves are receiving far more light than they can possibly use. The significance of the sunlit/shaded dichotomy decreases as diffuse light comes to dominate (Fig. 1b), as on hazy or cloudy days when the difference between sunlit and shaded irradiance is smaller. In the extreme

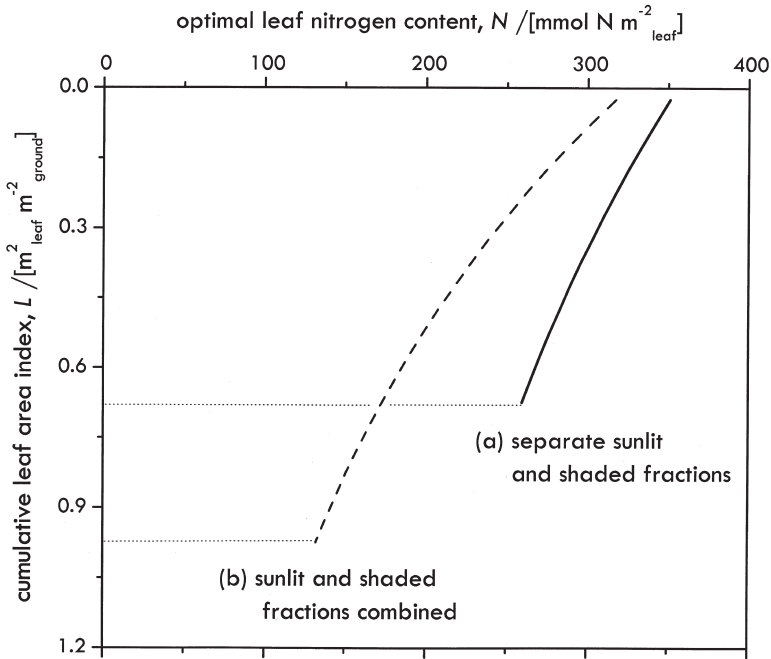


**Fig. 2.** Optimal canopy  $N$  profiles (relationships between leaf  $N$  content,  $N$ , and cumulative leaf area index,  $L$ ) inferred from a simulation in which separate sunlit and shaded irradiances were used (a, solid line), or the two irradiances were combined into a single irradiance in each layer (b, dashed line); the dotted horizontal lines represent the bottom of each canopy, and therefore their total LAI's ( $L_t$ ). The combined irradiance in (b) was equal to the sum of the sunlit and shaded values, weighted by the proportion of leaf area in each light fraction. Resource supplies were the same for both profiles ( $N_t = 211 \text{ mmol N m}^{-2}_{\text{ground}}$  and  $E_t = 511 \text{ mol H}_2\text{O m}^{-2}_{\text{ground}}$ ), so the areas under each profile are also the same (and equal to  $N_t$ ). (Simulations used the canopy light penetration model of de Pury and Farquhar (1997), with latitude =  $-20^\circ$ , longitude =  $152^\circ$ , day = 01 Jan, atmospheric transmissivity = 0.8, daylength = 13.2 h; air temperature ( $T_a$ ) varied sinusoidally between  $20^\circ\text{C}$  at sunrise to  $30^\circ\text{C}$  at solar noon.)

of a uniformly overcast sky (UOC) there is no beam light and the dichotomy disappears.

A multi-modal light environment also complicates prediction of optimal stomatal conductance. If sunflecks are sufficiently short, it is unlikely that stomata can respond fast enough to optimize gas exchange both for sunflecks and for 'shade-flecks' (continuous periods of time spent at the lower irradiance). Furthermore, models used for light penetration through canopies often make unrealistic assumptions about leaf morphology and leaf angle distributions. Deviations from these assumptions may have significant implications under certain conditions. For example, penumbral effects can dominate the character of light transmission within canopies with small

or narrow leaves like pine needles (Oker-Blom 1986), essentially eliminating the beam fraction at some depth in the canopy. Other aspects of canopy light penetration, such as spacing between trees and crown shape, may substantially affect the optimal profile of nitrogen when expressed as a function of cumulative leaf area index. If one wishes to generate nitrogen profiles that are directly, numerically testable, it may be necessary to use a more detailed and accurate treatment of canopy light penetration.

Fig. 2 demonstrates how inferred optimal  $N$  profiles might depend on whether the same total irradiance is distributed over one or two irradiance fractions. The profiles in Fig. 2 were calculated for the same values of  $N_t$  and  $E_t$ , but

one profile was inferred using a light model that distinguished between ‘sunlit’ and ‘shaded’ fractions of each canopy layer (de Pury and Farquhar 1997). For the other profile, the two light fractions were combined into a single value for each canopy layer, equal to a weighted average of the sunlit and shaded irradiances (the weights were the proportions of leaf area occupied by each light fraction in the sunlit/shaded model). The total absorbed irradiance of each layer was therefore identical for the two profiles. As Fig. 2 shows, when the same total irradiance is distributed between two irradiance fractions rather than one, the optimal profile has more nitrogen near the top of the canopy (and therefore less total leaf area as well).

### 3.3 One-Phase vs. Two-Phase Models of Leaf Photosynthesis

Many previous treatments of canopy nitrogen optimization used simplified models for photosynthesis – often a single hyperbolic function in which both nitrogen and light directly limit photosynthesis at all values of  $c_i$ , the intercellular CO<sub>2</sub> partial pressure (Caldwell et al. 1986, Hirose and Werger 1987, Gutschick and Wiegel 1988, Schieving et al. 1992, Schieving and Poorter 1999). However, at sufficiently low  $c_i$ , photosynthesis is limited by RuBP carboxylation, and therefore by Rubisco activity. Because Rubisco activity is limited by leaf nitrogen content but not directly by light, photosynthesis is essentially not light-limited at low values of  $c_i$ . Conversely, at high  $c_i$  the electron transport rate limits carbon flux through the Calvin cycle, and this process is limited by both nitrogen and light. Furthermore, the nitrogen dependencies of these two phases are quantitatively different, even when light is saturating (Evans 1983, Evans 1989). Fig. 3 shows how assimilation rate,  $A$  (Fig. 3a) and its marginal gain from N investment,  $\partial A/\partial N$  (Fig. 3b) vary with  $c_i$  for both of these phases. Also important is the relationship between  $c_i$  and  $k$ , the slope of the  $A$  vs  $c_i$  relationship (sometimes called ‘mesophyll conductance’). The value of  $k$  plays a central role in predicting optimal stomatal conductance, because  $k$  is a critical determinant of  $\lambda$  (Eq A40) (Cowan and

Farquhar 1977). Fig. 3c shows how  $k$  varies with  $c_i$  for the two phases of the model of Farquhar et al. (1980b). Two-phase models have a fundamentally different shape for  $k$  vs  $c_i$  than single-phase models because the shift from one phase to the other creates an inflection and translation (Fig. 3c), whereas the  $k$  vs.  $c_i$  curve for a single-phase model has uniformly positive curvature (cf. the curve marked ‘ $k_j$ ’ in Fig 3c). As a result,  $k$  is most sensitive to  $c_i$  (and therefore to stomatal conductance) at intermediate values of  $c_i$  in a two-phase model, but at low values in a single-phase model.

This distinction – two regimes in the response of photosynthetic capacity to nitrogen – dramatically impacts calculations related to the economy of nitrogen use. The two-phase treatment is particularly important for accurate analysis of nitrogen-water interactions, because the transition between these two phases is parameterized by  $c_i$ , which is affected by stomatal conductance and is therefore influenced by water use. (The model developed in the present paper uses the photosynthesis model of Farquhar et al. (1980b) to account for these two different regimes.) One potential error arises if the sunlit/shaded dichotomy is not taken into account when using a two-phase photosynthesis model. Fig. 3d shows the demand curve and the optimal supply line (defined by the optimal stomatal conductance) for each of two irradiances (300 and 1200  $\mu\text{mol photons m}^{-2} \text{s}^{-1}$ ). Imagine for a moment that this leaf actually spends half of its time at each of these two irradiances. Its average irradiance is therefore 750, and its average assimilation rate and stomatal conductance are the average of the high- and low-irradiance values. Imagine now that we wish to estimate gas exchange by calculating  $A$  and  $g_{sc}$  at the average irradiance of 750. Because photosynthesis in this leaf is nearly light-saturated at a irradiance 750, the demand curves at 750 and 1200 are very similar, and so are the optimal conductances. As Fig. 3d shows, the result would be an overestimation of the average values of both  $A$  and  $g_{sc}$  by more than 25%. This example demonstrates how it can be dangerous to mix levels of detail. It may seem intuitive that switching from a single-irradiance/single-phase model to a single-irradiance/two-phase model should improve the model’s accu-

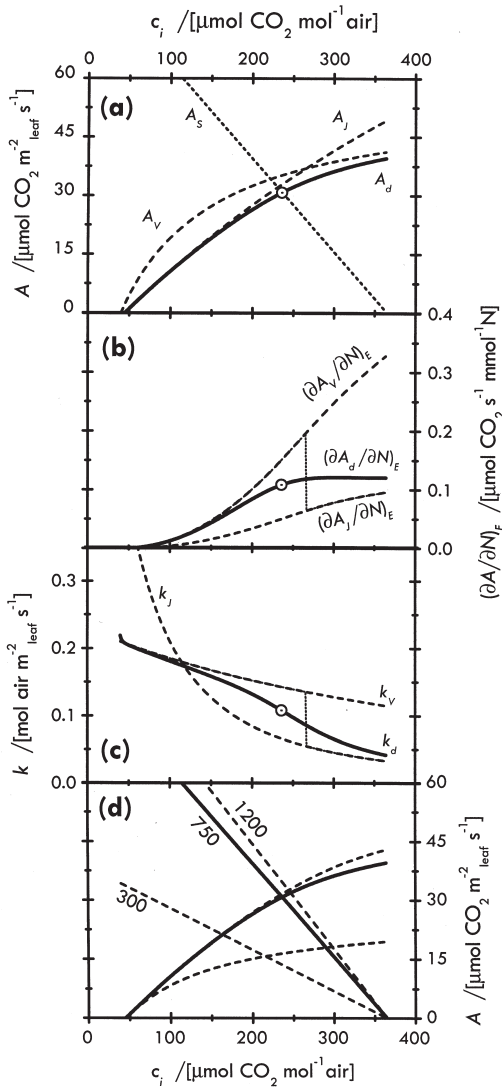


**Fig. 3.** (a) The photosynthesis model of Farquhar et al. (1980b): the Rubisco-limited and electron transport-limited phases ( $A_V$  and  $A_J$ , respectively; dashed lines), and the hyperbolic minimum of these two ( $A_d$ , solid line), for  $\theta_A = 0.98$ . Also shown is a ‘supply function’ ( $A_s$ , dotted line) for optimal stomatal conductance ( $\lambda = 0.5 \text{ mmol H}_2\text{O } \mu\text{mol}^{-1}\text{CO}_2$ ,  $N = 150 \text{ mmol m}^{-2}$ ,  $I = 750 \text{ } \mu\text{mol m}^{-2} \text{ s}^{-1}$ ,  $\theta_J = 0.7$ ,  $D = 20 \text{ mmol mol}^{-1}$ , and  $\omega = 1$ ), and an open circle indicating the intersection of the supply and demand functions. (b)  $(\partial A/\partial N)_E$  vs  $c_i$  for each phase (dashed lines) and for the smoothed transition (solid line is with  $\theta_A = 0.98$ ; the dotted line is an un-smoothed transition, with  $\theta_A = 1.0$ ), and the circle indicates the operating point on this curve for the optimal conductance in (a). (c)  $k$  (the slope of the demand curve:  $(\partial A_d/\partial c_i)_N$ ) vs  $c_i$  for each phase (dashed lines), for the smoothed transition (solid line,  $\theta_A = 0.98$ ) and the unsmoothed transition (dotted line,  $\theta_A = 1.0$ ). In a single-phase model, nitrogen and light would co-limit photosynthesis for all values of  $c_i$ , so the qualitative responses of  $(\partial A/\partial N)_E$  and  $k$  to  $c_i$  would be the same as those shown for the electron transport-limited phase of the two-phase model. (d) Demand curves for low and high irradiances (300 and 1200  $\mu\text{mol m}^{-2} \text{ s}^{-1}$ ), and for the average (750) of these two; the corresponding optimal supply curves (using the same conditions as in panel a) are also shown. The values of  $A$ ,  $c_i$ , and  $g_{sc}$  at the average irradiance are not equal to the average of their values at the low and high irradiances.

racy, but this assumption is not necessarily warranted.

### 3.4 Gradients of Nitrogen and Light within Leaves

Light attenuation occurs not only at the level of whole leaves, but also at a smaller scale within leaves (Terashima and Saeki 1983). Attenuation of light by chlorophyll creates a vertical gradient of irradiance within leaves (Terashima and Saeki

1983, Vogelmann et al. 1989, Cui et al. 1991, Han et al. 1999, Vogelmann and Han 2000). It is intuitively clear that more nitrogen should be allocated per unit of light-absorbing chlorophyll at the top of the leaf than at the bottom, but it is not clear how this allocation problem is actually solved in real leaves. This issue may appear to be of interest only to sub-leaf-scale physiologists. However, it has a dramatic impact on calculated optimal  $N$  profiles, because it determines how the whole-leaf potential electron transport rate ( $J$ , Eqs A9, A13, and A17) depends on leaf  $N$

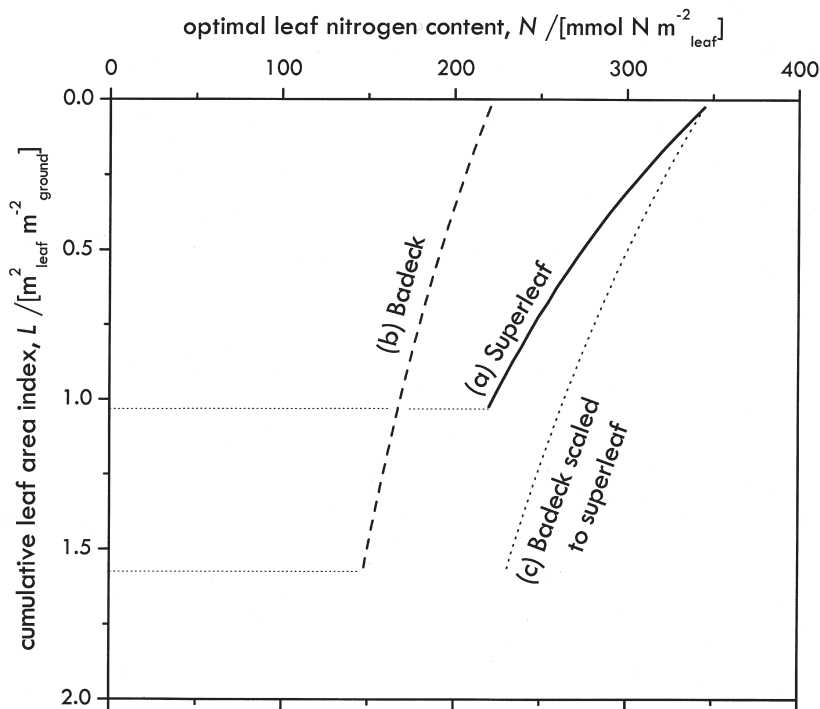


**Fig. 4.** Optimal canopy  $N$  profiles with whole-leaf potential electron transport rate ( $J$ ) calculated from (a, solid line) the ‘superleaf’-based model (Eqs A11–A13) and (b, dashed line) the model of Badeck (1995) (Eqs A14–A17); the *horizontal* dotted lines represent the bottom of each canopy, and therefore their total LAI’s ( $L_t$ ). Resource supplies were the same for both profiles ( $N_t = 288 \text{ mmol N m}^{-2}_{\text{ground}}$  and  $E_t = 638 \text{ mol H}_2\text{O m}^{-2}_{\text{ground}}$ ). The dotted profile (curve c) is the Badeck-based profile, re-scaled to have the same value of  $N$  at  $L = 0$  as the superleaf-based profile, in order to show that the superleaf curve declines more steeply than the Badeck curve. (Simulations used the canopy light penetration model of de Pury and Farquhar (1997), with parameters as for Fig. 2).

content ( $N$ ) and incident irradiance ( $I$ ). Fig. 4 shows optimal  $N$  profiles inferred using two different models (described below) to predict  $J$  from  $N$  and  $I$ .

One hypothesis is that  $N$  is allocated among ‘layers’ of chlorophyll in direct proportion to the irradiance absorbed by each layer within the leaf. This idea is an extension of the ‘superleaf’ hypothesis (Field 1991), which states that light and nitrogen are equally limiting everywhere in a plant. The standard model for  $J$  (Eqs A11–A3) is implicitly based on this hypothesis, because it does not distinguish between layers in the leaf. However, at low irradiances, fewer photons are absorbed every second per unit of chlorophyll (and hence per unit of  $N$  invested in light capture), even though each photon can drive the same

electron flow per unit of  $N$  invested in electron transport. To account for the nitrogen cost of light capture, Badeck (1995) formalized an alternative model (Eqs A14–A17; Fig. 5). In contrast to the standard model, Badeck’s model assumes there is no  $N$  gradient within the leaf, so chloroplasts near the sunlit surface of the leaf are more nitrogen-limited than those near the bottom of the leaf (Fig. 5).

The weight of empirical evidence suggests that, under controlled conditions, leaves allocate nitrogen internally in parallel to the light gradient (e.g., Ogren and Evans 1993, Evans 1995, Evans 1999), consistent with the superleaf-based model. However, leaves that flicker or rotate rapidly (e.g., *Populus tremuloides*), or are oriented vertically, may be just as likely to receive irradiance from

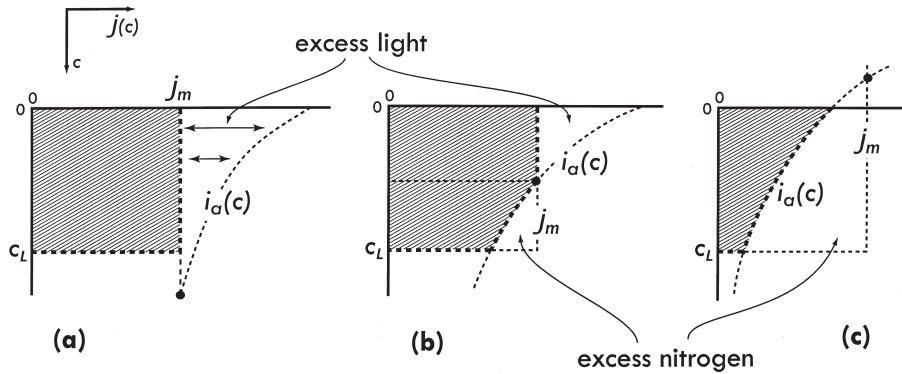


**Fig. 5.** Diagram illustrating the model of Badeck (1995) for electron transport rate (Eqs A14–A17). The vertical axis in each plot represents cumulative chlorophyll content ( $c$  / [mmol Chl  $m^{-2}$ ]), so the diagram's orientation is similar to a transdermal leaf section;  $c_L$ , the total leaf Chl content, corresponds to the bottom of the leaf. The horizontal axis represents the potential electron rate per unit of chlorophyll ( $j(c)$ ), and components thereof ( $j_m$ , the N-limited component, and  $i_a(c)$ , the light-limited component).  $J$  equals the shaded area in each plot. At some value of  $c$ , N and light would be perfectly co-limiting ( $j_m = i_a$ , represented by the solid dark circles), but this may occur either above, within, or below the leaf; these three cases are represented by panels (a), (b) and (c), respectively. In (a) and (b), some light is absorbed but not used, because the electron transport capacity is saturated in some layers; conversely, in (b) and (c) some nitrogen is not fully utilized, because the local irradiance is too low.

either surface; in such leaves, a monotonic internal N gradient might be less efficient than no gradient at all, in which case Badeck's model would be more appropriate than the standard superleaf-based model. Finally, within-leaf light gradients may change when leaves are illuminated by diffuse irradiance rather than by collimated or 'beam' irradiance (Ustin et al. 2001), further confusing the issue. More study seems to be warranted on this topic.

### 3.5 Effects of Leaf Temperature

Many previous analyses of canopy nitrogen allocation have assumed leaf temperature to be constant for simplicity (e.g., Hirose and Werger 1987, Gutschick and Wiegand 1988, Werger and Hirose 1991, Schieving and Poorter 1999). However, nitrogen and water are tightly linked by thermal effects, because changes in leaf temperature ( $T_l$ ) caused by transpiration (via evaporative cooling) can significantly affect the performance of photosynthetic enzymes (Farquhar et al. 1980b, Brooks and Farquhar 1985, Harley et al. 1992,

Bernacchi et al. 2001), which in turn affects the use-efficiency of nitrogen invested in those enzymes. The resulting effects are not easy to intuit. First, variations in  $T_l$  around a baseline value can either increase or decrease photosynthetic performance, depending on whether the baseline is above or below the optimum. Second, the effect of transpiration on  $T_l$  is likely to increase with depth in the canopy, because lower leaves are more sheltered from convective heat exchange with the atmosphere than are upper leaves (Roberts et al. 1990). Third, it is possible for  $T_l$  effects to critically change the topology of the relationships between assimilation rate and transpiration rate (Cowan and Farquhar 1977, Buckley et al. 1999), which in turn affects the mathematics of optimization. A full iterative solution of leaf energy balance and a treatment of intracanopy aerodynamics should help to account for these effects. Optimal N profiles can be predicted with and without these details to estimate the importance of thermal effects. For example, Fig. 6 compares an optimal canopy N profile in which  $T_l$  was determined by iterative solution of an energy balance formula (Eq A19), with the

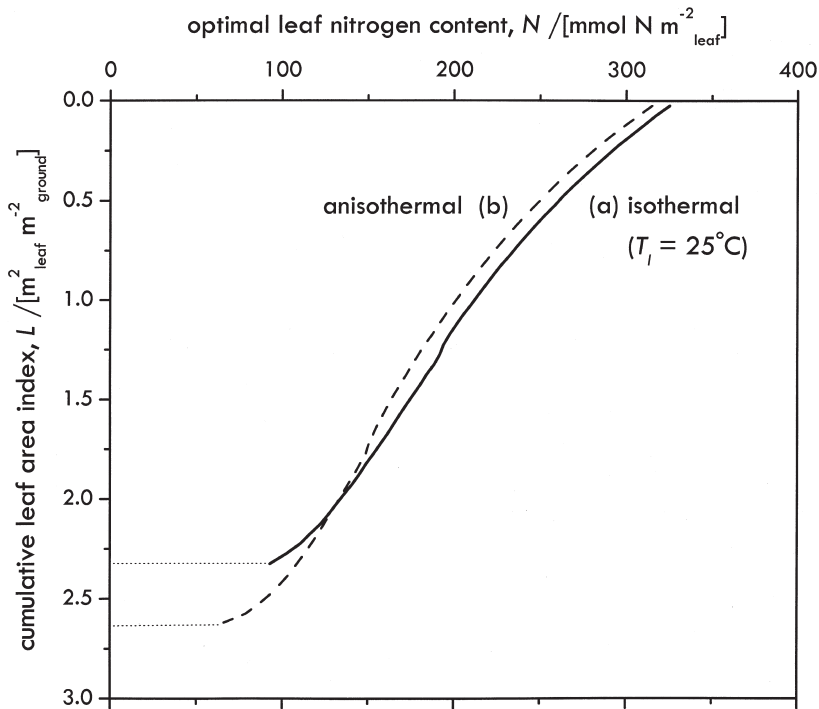


**Fig. 6.** Optimal canopy  $N$  profiles with leaf temperature ( $T_l$ ) either forced to equal  $25^\circ\text{C}$  (a, solid line, ‘isothermal’), or determined by iterative solution of an energy balance expression (Eq A19) (b, dashed line, ‘anisothermal’). Resource supplies were the same for both profiles ( $N_t = 487 \text{ mmol N m}^{-2}_{\text{ground}}$  and  $E_t = 1086 \text{ mol H}_2\text{O m}^{-2}_{\text{ground}}$ ). (Simulations used the canopy light penetration model of de Pury and Farquhar (1997), with parameters as for Fig. 2).

profile predicted for the same resource supplies when  $T_l$  was set equal to  $25^\circ\text{C}$ . The isothermal profile has higher leaf  $N$  contents in each layer, and as a result, its total LAI is lower, because the  $N$  supply is more concentrated in upper layers.

## 4 Discussion and Conclusions

The purpose of this paper was to develop a theoretical and mathematical framework for studying linked optimization of canopy nitrogen allocation and water use. In this section, we summarize the analyses and conclusions of the preceding sections, we suggest questions that may be addressed by this framework, and we conclude with a brief discussion of the role of optimality theory in plant ecophysiology.

### 4.1 Summary

We have stated the abstract mathematical solution for optimal water and nitrogen use in an individual plant canopy. Simply, the general solution is that net carbon gain should respond by the same amount, in any leaf, to a small increase in resource investment – the ‘marginal gain,’ to use economic terminology, should be constant and uniform. This is true for both water and nitrogen investments, but for nitrogen, the relevant timescale should average net carbon gain over a day or more (because nitrogen cannot be translocated very rapidly). However, although the numerical values of these marginal gains (denoted  $\lambda$  and  $\eta$  for water and nitrogen, respectively) are constant *within* an optimal plant, they are not, in general, constant over any broader domains. For example,  $\lambda$  and  $\eta$  will differ among plants with

different water and nitrogen supplies ( $E_t$  and  $N_t$ , respectively), different physical environments (e.g. radiation regimes, humidity, carbon dioxide supply, and air temperature), or different physiological constraints (e.g.,  $C_3$  vs  $C_4$  photosynthetic pathways).

Several factors must be considered when attempting to infer optimal resource use strategies – i.e., when attempting to translate values of  $\lambda$  and  $\eta$  into patterns of water and nitrogen use within a plant. For example, to find the values of stomatal conductance ( $g_{sc}$ ) and leaf N content ( $N$ ) that produce the correct  $\lambda$  and  $\eta$ , many ‘candidate’ values of  $g_{sc}$  and  $N$  must be compared. This is accomplished by calculating the appropriate marginal gain at each candidate value. However, the marginal gains are partial derivatives in which some variables must be held constant while others are allowed to vary. Candidate  $g_{sc}$  values must be compared at the same  $N$  and incident irradiance, but anything directly affected by  $g_{sc}$  (including transpiration rate, and therefore leaf temperature and photosynthetic parameters) must be allowed to vary among candidate  $g_{sc}$  values. Candidate  $N$  values must allow  $g_{sc}$  (and anything directly affected by it) to vary, because in practice, stomata respond to things affected by  $N$  (such as photosynthetic capacity) much more quickly than  $N$  itself can change. (However, further mathematical analysis shows that this latter requirement can be dropped if water use is known to be optimal.) In the Appendix, we have derived general formulas for these marginal gains, using a standard model of leaf gas exchange and energy balance.

Some physiological and physical factors can significantly affect the optimal resource use strategies inferred from any particular model. These include: (a) the use of a canopy light penetration model that accounts for sunlit and shaded fractions of each canopy layer (or more generally, for more complex penumbral effects), (b) the use of a biphasic photosynthesis model, in which the economies of nitrogen and water use depend differently on intercellular  $CO_2$  partial pressure ( $c_i$ ) in each phase, (c) the model chosen for whole-leaf potential electron transport rate, on the basis of hypotheses concerning nitrogen and light gradients within leaves, and (d) the effects, on leaf temperature, of evaporative cooling and variation of convective coupling with depth in the

canopy. We used preliminary simulations to demonstrate the potential effects of these factors on inferred canopy N profiles (using a complete canopy model that is not presented here). Future work will investigate these factors in depth.

## 4.2 Possible Applications of the Mathematical Framework

Rigorous analysis of resource-use efficiency and interactions between resources, facilitated by the mathematical framework developed in this study, can help investigators interpret and predict characteristics of gas exchange. This is not a trivial problem because the response of carbon gain to the investment of any single resource depends on scale, and on the status of other limiting resources. Ideally, the efficiency with which a resource is used should be measured at a scale where the resource limitation is uniquely defined. For example, water use efficiency (the ratio of carbon gain to water use) is often inferred from its relationship to certain measurable small-scale quantities, such as leaf gas exchange variables or carbon isotope discrimination signals in isolated tissues (Farquhar and Richards 1984). However, because resource constraints apply at the scale of whole plants, rather than individual leaves, an arbitrarily localized proxy measurement for water- or nitrogen-use efficiency (WUE or NUE) will not necessarily be uniquely related to the associated canopy-scale efficiency. For example, a set of trees may be ranked in a certain order with respect to whole-tree WUE ( $A_t/E_t$ ), but the local WUE ( $A/E$ ) measured in upper-canopy leaves may rank the trees differently. Similarly, stomatal conductance is known to be correlated with photosynthetic capacity along some domains (Wong et al. 1979), but the sense of those correlations need not hold among parallel loci in different canopies.

The mathematical framework developed in this paper can be used to predict relationships between various whole-plant and individual-leaf-scale properties of gas exchange, in order to identify easily-measured but robust estimators of the large-scale properties of interest. This model may also be able to predict useful relationships among whole-canopy variables such as assim-

ilation rate, leaf area index, and water and nitrogen supplies. Any relationships predicted for canopy-scale variables could help explain observed ecological patterns, or predict patterns not yet observed. Furthermore, relationships linking whole-plant carbon gain to whole-plant resource supplies could become powerful scaling tools, because they would allow gross primary productivity to be easily predicted from mappable data that are related to resource limitations (e.g., soil parent material, site water balance, or NDVI).

### 4.3 Optimization as an Alternative to Traditional Reduction

It is our view that optimality can be a powerful paradigm for constructing ecological models. As an ecological principle for predicting or interpreting plant gas exchange, optimality derives its utility mainly from two features. First, identifying an optimal pattern reduces the system of interest to a small number of degrees of freedom by eliminating the infinite complement of suboptimal patterns. Second, an optimal pattern represents a logical extreme towards which phenotypes in the natural system under study may be reasonably *hypothesized* to have evolved. In other words, optimization uses the closest thing biology has to a scientific law – natural selection – to distill a complex system into an essential kernel of arbitrary simplicity. This kernel can then be used as a basis in the truest mathematical sense.

However, simplification, or the elimination of complexity, is more commonly achieved in science by analytical reduction (i.e., linearisation of mathematical models, which assumes complex dynamics do not emerge from essential aspects of mechanisms), empirical reduction (elimination of noise by statistical modeling, which assumes complexity is random), or scale reduction (identification of some arbitrarily small scale as the unique locus of mechanistic control, and ignoring processes that only arise, and are thus only defined, at larger scales). Reduction is, in some sense, the mother of all null models. Not only does it simplify; it demystifies the process of simplification so much that it is the first recourse of investigators faced with a complicated system.

In other words, reduction has become an implicit paradigm. This is probably due in part to its success in other sciences (many physical systems are often well-described by a linear basis that is polluted only by random variation or by fundamentally separable systematic effects), but it is also popular because it is conceptually simple.

Consider, for example, Brownian motion. While certainly interesting as an emergent phenomenon, it can be described by a few physical laws that apply universally to each member of an enormous population of essentially identical objects. That is, the dynamics of particles are created by interactions that are external to those particles, so the two features – object and force – can be mathematically separated and thus described by a linear basis. A canopy of leaves, on the other hand, may be a collection of essentially similar objects in some respects, but an understanding of canopy properties requires consideration of the whole canopy as a single coordinated object with internal dynamics. (In the canopy, internal coordination derives from the need for leaves to share a common resource pool). Therefore, if the goal is to understand canopy-level phenomena, it is not sufficient to divide the canopy into independent units of a defined scale. Those units must be integrated by metascale processes, such as the allocation of a common resource pool.

Were there no resource limitation, the canopy would have neither reason nor power to tyrannize its citizen leaves. It is the force of competition (interspecific, intraspecific, or even intrasomal) and the constraints of history (chiefly genetics and environmental change) that ecology adds to the sometimes separable forces of physical law. This renders biological dynamics *essentially* nonlinear. Thus linearisation may be not only inadequate, but quite inappropriate as a tool for simplifying biological systems. Optimization, despite its own bugaboos, may be a more viable tool.

Furthermore, many physical systems are quite interesting at equilibrium, when linear models are most unassailable; at worst, their equilibrium behavior is often explained by forces in the direction of an unambiguous equilibrium state. Ecological systems, on the other hand, are fundamentally historical – they generally have no meaningful equilibrium or steady-state condition.

This may be partly because their internal dynamics are very complicated (in which case there may be many relatively unstable equilibrium), and it may also be because they are embedded in a much larger system with complex dynamics across many scales of space and time (in which case there may be no equilibrium at all). The present state of an ecological system often makes sense only in the context of a convincing story explaining how that state came to be.

One may justifiably argue that in implementing optimization, we employ reductionist techniques. Ironically, this argument, in its logical dissolution, clarifies our thesis. It is true that we write down simple equations based on separation of processes – we linearise the physical system at some scales. However, we also link these processes with physical models of their interactions, thereby explicitly *integrating* these processes. Where reduction fails is as a tool for interpreting the behavior of these integrated models. Many ecologically important phenomena will be lost or misinterpreted if we attempt to simply the behavior of an integrated system by reduction, i.e., dis-integration. Optimality offers another method of finding the *essence* of a natural system – the modal behavior from which it tends to deviate unpredictably and perhaps meaninglessly – while preserving the historical basis of all long-term biological dynamics: natural selection.

## References

- Amthor, J.S., Goulden, M.L., Munger, J.W. & Wofsy, S.C. 1994. Testing a mechanistic model of forest-canopy mass and energy exchange using eddy correlation: carbon dioxide and ozone uptake by a mixed-oak stand. *Australian Journal of Plant Physiology* 21: 623–651.
- Badeck, F.-W. 1995. Intra-leaf gradient of assimilation rate and optimal allocation of canopy nitrogen: a model on the implications of the use of homogeneous assimilation functions. *Australian Journal of Plant Physiology* 22: 425–439.
- Bernacchi, C.J., Singaas, E.L., Pimentel, C., Portis, A.R.J. & Long, S.P. 2001. Improved temperature response functions for models of Rubisco-limited photosynthesis. *Plant, Cell and Environment* 24: 253–259.
- Berninger, F., Mäkelä, A. & Hari, P. 1996. Optimal control of gas exchange during drought: empirical evidence. *Annals of Botany* 77: 469–476.
- Brooks, A. & Farquhar, G.D. 1985. Effect of temperature on the CO<sub>2</sub>/O<sub>2</sub> specificity of Ribulose-1,5-bisphosphate carboxylase/oxygenase and the rate of respiration in the light. Estimates from gas-exchange measurements on spinach. *Planta* 165: 397–406.
- Buckley, T.N., Farquhar, G.D. & Mott, K.A. 1999. Carbon-water balance and patchy stomatal conductance. *Oecologia* 118: 132–143.
- Caemmerer, S.v., Evans, J.R., Hudson, G.S. & Andrews, T.J. 1994. The kinetics of ribulose-1,5-bisphosphate carboxylase/oxygenase in vivo inferred from measurements of photosynthesis in leaves of transgenic tobacco. *Planta* 195: 88–97.
- Caldwell, M.M., Meister, H.-P., Tenhunen, J.D. & Lange, O.L. 1986. Canopy structure, light microclimate and leaf gas exchange of *Quercus coccifera* L. in a Portuguese macchia: measurements in different canopy layers and simulations with a canopy model. *Trees* 1: 25–41.
- Cordell, S., Goldstein, G., Meinzer, F.C. & Handley, L.L. 1999. Allocation of nitrogen and carbon in leaves of *Metrosideros polymorpha* regulates carboxylation capacity and δ<sup>13</sup>C along an altitudinal gradient. *Functional Ecology* 13: 811–818.
- Cowan, I.R. 1977. Stomatal behaviour and environment. *Advances in Botanical Research* 4: 117–228.
- 1982. Water use and optimization of carbon assimilation. In: Lange, O.L., Nobel, C.B., Osmond, C.B. & Ziegler, H. (eds.). *Encyclopedia of plant physiology*. 12B. Physiological plant ecology. Springer-Verlag, Berlin. p. 589–630.
- 1986. Economics of carbon fixation in higher plants. In: Givnish, T.J. (ed.) *On the economy of plant form and function*. Cambridge University Press, Cambridge. p. 133–170.
- & Farquhar, G.D. 1977. Stomatal function in relation to leaf metabolism and environment. *Symposium of the Society for Experimental Biology* 31: 471–505.
- Cui, M., Vogelmann, T.C. & Smith, W.K. 1991. Chlorophyll and light gradients in sun and shade leaves of *Spinacia oleracea*. *Plant, Cell and Environment* 14: 493–500.
- de Pury, D.G.G. & Farquhar, G.D. 1997. Simple scaling of photosynthesis from leaves to canopies with-

- out the errors of big-leaf models. *Plant, Cell and Environment* 20: 537–557.
- Evans, J.R. 1983. Nitrogen and photosynthesis in the flag leaf of wheat (*Triticum aestivum* L.). *Plant Physiology* 72: 297–302.
- 1989. Photosynthesis and nitrogen relationships in leaves of C3 plants. *Oecologia* 78: 9–19.
- 1993. Photosynthetic acclimation and nitrogen partitioning within a lucerne canopy. II. Stability through time and comparison with a theoretical optimum. *Australian Journal of Plant Physiology* 20: 69–82.
- 1995. Carbon fixation profiles do reflect light absorption profiles in leaves. *Australian Journal of Plant Physiology* 22: 865–873.
- 1999. Leaf anatomy enables more equal access to light and CO<sub>2</sub> between chloroplasts. *New Phytologist* 143: 93–104.
- Farquhar, G.D. 1989. Models of integrated photosynthesis of cells and leaves. *Philosophical Transactions of the Royal Society of London, Series B* 323: 357–367.
- & Richards, R.A. 1984. Isotopic composition of plant carbon correlates with water-use efficiency of wheat genotypes. *Australian Journal of Plant Physiology* 11: 539–552.
- & Sharkey, T.D. 1982. Stomatal conductance and photosynthesis. *Annual Review of Plant Physiology* 33: 317–345.
- , Schulze, E.D. & Koppers, M. 1980a. Responses to humidity by stomata of *Nicotiniana glauca* L. and *Corylus avellana* L. are consistent with the optimization of carbon dioxide uptake with respect to water loss. *Australian Journal of Plant Physiology* 7: 315–327.
- , von Caemmerer, S. & Berry, J.A. 1980b. A biochemical model of photosynthetic CO<sub>2</sub> assimilation in leaves of C3 species. *Planta* 149: 78–90.
- , Buckley, T.N. & Miller, J.M. 2002. Optimal stomatal control in relation to leaf area and nitrogen content. *Silva Fennica* 36(3): 625–637. (this issue)
- Field, C. 1983. Allocating leaf nitrogen for the maximization of carbon gain: leaf age as a control on the allocation program. *Oecologia* 56: 341–347.
- & Mooney, H.A. 1986. The photosynthesis-nitrogen relationship in wild plants. In: Givnish, T.J. (ed.) *On the economy of plant form and function*. Cambridge University Press, Cambridge. p. 25–55.
- , Merino, J. & Mooney, H.A. 1983. Compromises between water-use efficiency and nitrogen-use efficiency in five species of California evergreens. *Oecologia* 60: 384–389.
- Field, C.B. 1991. Ecological scaling of carbon gain to stress and resource availability. In: Mooney, H.A., Winner, W.E. & Pell, E.J. (eds.) *Response of Plants to Multiple Stresses*. Academic Press, San Diego. p. 35–65.
- Givnish, T.J. 1986. Introduction. In: Givnish, T.J. (ed.) *On the economy of plant form and function*. Cambridge University Press, Cambridge. p. 1–9.
- Gonzales-Real, M.M. & Baille, A. 2000. Changes in leaf photosynthetic parameters with leaf position and nitrogen content within a rose plant canopy (*Rosa hybrida*). *Plant, Cell and Environment* 23: 351–363.
- Gutschick, V.P. & Wiegel, F.W. 1988. Optimizing the canopy photosynthetic rate by patterns of investment in specific leaf mass. *The American Naturalist* 132: 67–86.
- Han, T., Vogelmann, T.C. & Nishio, J.N. 1999. Profiles of photosynthetic oxygen-evolution within leaves of *Spinacia oleracea*. *New Phytologist* 143: 83–92.
- Hari, P., Mäkelä, A., Berninger, F. & Pohja, T. 1999. Field evidence for the optimality hypothesis of gas exchange in plants. *Australian Journal of Plant Physiology* 26: 239–244.
- , Mäkelä, A. & Pohja, T. 2000. Surprising implications of the optimality hypothesis of stomatal regulation gain support in a field test. *Australian Journal of Plant Physiology* 27: 77–80.
- , Nilson, T., Salminen, R., Kaipainen, L., Korpilahti, E. & Ross, J. 1984. Nonlinear dependence of photosynthetic rate on irradiance and its consequences for estimation of saccharides formed. *Photosynthetica* 18: 28–33.
- Harley, P.C., Thomas, R.B., Reynolds, J.F. & Strain, B.R. 1992. Modelling photosynthesis of cotton grown in elevated CO<sub>2</sub>. *Plant, Cell and Environment* 15: 271–282.
- Hirose, T. & Werger, M.J.A. 1987. Maximizing daily canopy photosynthesis with respect to the leaf nitrogen allocation pattern in the canopy. *Oecologia* 72: 520–526.
- Korpilahti, E. 1988. Photosynthetic production of Scots pine in the natural environment. *Acta Forestalia Fennica* 202: 1–71.
- Koskela, J., Hari, P. & Pipatwattanakul, D. 1999. Anal-

- ysis of gas exchange of Merkus pine populations by the optimality approach. *Tree Physiology* 19: 511–518.
- Leuning, R., Kelliher, F.M., de Pury, D.G.G. & Schulze, E.D. 1995. Leaf nitrogen, photosynthesis, conductance and transpiration: scaling from leaves to canopies. *Plant, Cell and Environment* 18: 1183–1200.
- Lloyd, J., Grace, J., Miranda, A.C., Meir, P., Wong, S.C., Miranda, H.S., Wright, I.R., Gash, J.H.C. & McIntyre, J. 1995. A simple calibrated model of Amazon rainforest productivity based on leaf biochemical properties. *Plant, Cell and Environment* 18: 1129–1145.
- Mäkelä, A., Berninger, F. & Hari, P. 1996. Optimal control of gas exchange during drought: theoretical analysis. *Annals of Botany* 77: 461–467.
- Ogren, E. & Evans, J.R. 1993. Photosynthetic light response curves. I. The influence of CO<sub>2</sub> partial pressure and leaf inversion. *Planta* 189: 182–190.
- Oker-Blom, P. 1986. Photosynthetic radiation regime and canopy structure in modeled forest stands. *Acta Forestalia Fennica* 187: 1–44.
- Pearcy, R.W. 1990. Sunflecks and photosynthesis in plant canopies. *Annual Review of Plant Physiology* 41: 421–453.
- Reich, P.B., Walters, M.B. & Tabone, T.J. 1989. Response of *Ulmus americana* seedlings to varying nitrogen and water status. 2. Water and nitrogen use efficiency. *Tree Physiology* 5: 173–184.
- Roberts, J., Cabral, O.M.R. & de Aguiar, L.F. 1990. Stomatal and boundary-layer conductances in an Amazonian terra firme rain forest. *Journal of Applied Ecology* 27: 336–353.
- Schieving, F. & Poorter, H. 1999. Carbon gain in a multispecies canopy: the role of specific leaf area and photosynthetic nitrogen-use efficiency in the tragedy of the commons. *New Phytologist* 143: 201–211.
- , Werger, M.J.A. & Hirose, T. 1992. Canopy structure, nitrogen distribution and whole canopy photosynthetic carbon gain in growing and flowering stands of tall herbs. *Vegetatio* 102: 173–181.
- Sellers, P.J., Berry, J.A., Collatz, G.J., Field, C.B. & Hall, F.G. 1992. Canopy reflectance, photosynthesis and transpiration. III: A reanalysis using improved leaf models and a new canopy integration scheme. *Remote Sensing of the Environment* 42: 187–216.
- Smolander, H. 1984. Measurement of fluctuating irradiance in field studies of photosynthesis. *Acta Forestalia Fennica* 187: 1–56.
- Terashima, I. & Saeki, T. 1983. Light environment within a leaf. I. Optimal properties of paradermal sections of *Camellia* leaves with special reference to differences in the optical properties of palisade and spongy tissues. *Plant and Cell Physiology* 24: 1493–1501.
- Ustin, S.L., Jacquemoud, S. & Govaerts, Y. 2001. Simulation of photon transport in a three-dimensional leaf: implications for photosynthesis. *Plant, Cell and Environment* 24: 1095–1103.
- Vogelmann, T.C. & Han, T. 2000. Measurement of gradients of absorbed light in spinach leaves from chlorophyll fluorescence profiles. *Plant, Cell and Environment* 23: 1303–1311.
- , Bornman, J.F. & Jossierand, S. 1989. Photosynthetic light gradients and spectral regime within leaves of *Medicago sativa*. *Philosophical Transactions of the Royal Society of London, Series B* 323: 411–421.
- Wan, F.Y.M. 1995. Introduction to the calculus of variations and its applications. Chapman and Hall, New York. 638 p.
- Werger, M.J.A. & Hirose, T. 1991. Leaf nitrogen distribution and whole canopy photosynthetic carbon gain in herbaceous stands. *Vegetatio* 97: 11–20.
- Wong, S.C., Cowan, I.R. & Farquhar, G.D. 1979. Stomatal conductance correlates with photosynthetic capacity. *Nature* 282: 424–426.

*Total of 60 references*

## Appendix

In this Appendix, we derive general expressions for the marginal gains ( $\partial A/\partial E$  and  $\partial A/\partial N$ , invariance of which specifies an optimal resource use strategy; see Section 2 in the main text) from a formal model of leaf gas exchange. The model is presented only in enough detail to allow this derivation. (A more complete model, which included detailed submodels of canopy light penetration model and intracanopy aerodynamics (Leuning et al. 1995, de Pury and Farquhar 1997), was used to generate the figures. However, because these figures are intended solely to demonstrate how the physiological phenomena discussed in Section 3 might affect inferred optimal canopy N profiles, we do not present this simulation model in full.) All parameters and variables are presented in Tables 1 and 2 with descriptions and units. Parameter values used to generate the figures are presented in the figure legends or in Table 3.

**Table 1.** General parameters and variables.

| Symbol                         | Name   | Units  |
|--------------------------------|--|--|
| $A$                            | net CO <sub>2</sub> assimilation rate of leaf                                  | $\mu\text{mol CO}_2 \text{ m}^{-2}_{\text{leaf}} \text{ s}^{-1}$   |
| $E$                            | transpiration rate of leaf   | $\text{mmol H}_2\text{O m}^{-2}_{\text{leaf}} \text{ s}^{-1}$      |
| $N$                            | leaf functional N content  | $\text{mmol N m}^{-2}_{\text{leaf}}$                               |
| $g_{sc}$ ( $g_{sw}$ )          | stomatal conductance to CO <sub>2</sub> (H <sub>2</sub> O)                     | $\text{mol air m}^{-2}_{\text{leaf}} \text{ s}^{-1}$               |
| $L$                            | cumulative leaf area index   | $\text{m}^2_{\text{leaf}} \text{ m}^{-2}_{\text{ground}}$          |
| $t$                            | time   | s  |
| $A_t$                          | net CO <sub>2</sub> assimilation rate of plant                                 | $\mu\text{mol CO}_2 \text{ m}^{-2}_{\text{ground}} \text{ s}^{-1}$ |
| $E_t$                          | transpiration rate of plant  | $\text{mmol H}_2\text{O m}^{-2}_{\text{ground}} \text{ s}^{-1}$    |
| $N_t$                          | plant functional N content   | $\text{mmol N m}^{-2}_{\text{ground}}$                             |
| $L_t$                          | whole-plant cumulative leaf area index   | $\text{m}^2_{\text{leaf}} \text{ m}^{-2}_{\text{ground}}$          |
| $\lambda$                      | invariant value of $(pE/pA)_N$ in optimal plant                                | $\text{mmol H}_2\text{O } \mu\text{mol}^{-1}\text{CO}_2$           |
| $\eta$                         | invariant value of $pN/pA$ in optimal plant                                    | $\text{mmol N } \mu\text{mol}^{-1}\text{CO}_2 \text{ s}$           |
| $\nu$                          | invariant value of $(pN/pA)_E$ in optimal plant                                | $\text{mmol N } \mu\text{mol}^{-1}\text{CO}_2 \text{ s}$           |
| $A_d$                          | biochemical demand function for $A$  | $\mu\text{mol CO}_2 \text{ m}^{-2}_{\text{leaf}} \text{ s}^{-1}$   |
| $A_s$                          | diffusional supply function for $A$  | $\mu\text{mol CO}_2 \text{ m}^{-2}_{\text{leaf}} \text{ s}^{-1}$   |
| $A_v$                          | RuBP carboxylation-limited expression for $A_d$                                | $\mu\text{mol CO}_2 \text{ m}^{-2}_{\text{leaf}} \text{ s}^{-1}$   |
| $A_j$                          | RuBP regeneration-limited expression for $A_d$                                 | $\mu\text{mol CO}_2 \text{ m}^{-2}_{\text{leaf}} \text{ s}^{-1}$   |
| $\hat{\lambda}$                | $pE/pA$ at constant $c_i$  | $\text{mmol H}_2\text{O } \mu\text{mol}^{-1}\text{CO}_2$           |
| $\hat{\eta}$ ( $= \hat{\nu}$ ) | $pN/pA$ at constant $c_i$  | $\text{mmol N } \mu\text{mol}^{-1}\text{CO}_2 \text{ s}$           |
| $\zeta$                        | invariant value of $dN/dE$ in plant with both water and nitrogen use optimised | $\text{mmol H}_2\text{O mmol}^{-1}\text{N}$                        |
| $T_l$ ( $T_a$ )                | leaf (air) temperature   | K  |
| $g_{bc}$ ( $g_{bw}$ )          | boundary layer conductance to CO <sub>2</sub> (H <sub>2</sub> O)               | $\text{mol air m}^{-2}_{\text{leaf}} \text{ s}^{-1}$               |
| $g_{tc}$ ( $g_{tw}$ )          | total conductance to CO <sub>2</sub> (H <sub>2</sub> O)                        | $\text{mol air m}^{-2}_{\text{leaf}} \text{ s}^{-1}$               |
| $\omega$                       | $dg_{tc}/dg_{tw}$  | unitless   |
| $g_{bh}$                       | boundary layer conductance to heat   | $\text{mol air m}^{-2}_{\text{leaf}} \text{ s}^{-1}$               |
| $c_i$ ( $c_a$ )                | intercellular (ambient) CO <sub>2</sub> mole fraction                          | $\mu\text{mol CO}_2 \text{ mol}^{-1}\text{air}$                    |
| $w_i$ ( $w_a$ )                | intercellular (ambient) H <sub>2</sub> O mole fraction                         | $\text{mmol H}_2\text{O mol}^{-1}\text{air}$                       |

**Table 2.** Parameters and variables of the biochemical photosynthesis model.

| Symbol  | Name   | Units   |
|---|--|---|
| $V_m$   | maximum RuBP carboxylation rate  | $\mu\text{mol CO}_2 \text{ m}^{-2}_{\text{leaf}} \text{ s}^{-1}$                |
| $J$   | potential electron transport rate  | $\mu\text{mol e}^- \text{ m}^{-2}_{\text{leaf}} \text{ s}^{-1}$                 |
| $J_m$   | maximum potential electron transport rate  | $\mu\text{mol e}^- \text{ m}^{-2}_{\text{leaf}} \text{ s}^{-1}$                 |
| $I_a$   | useful irradiance absorbed by PSII ( $\alpha FI$ )   | $\mu\text{mol photons m}^{-2}_{\text{leaf}} \text{ s}^{-1}$                     |
| $\alpha$  | leaf absorptance   | unitless  |
| $I$   | irradiance (photosynthetic photon flux density at leaf surface)                                  | $\mu\text{mol photons m}^{-2}_{\text{leaf}} \text{ s}^{-1}$                     |
| $F$   | (fraction of $\alpha I$ absorbed by PSII)(quantum yield)   | unitless  |
| $\theta_A$ ( $\theta_J$ )   | colimitation factors:<br>$A_d = \min\{A_v, A_j, \theta_A\}$ ( $J = \min\{J_m, I_a, \theta_J\}$ ) | unitless  |
| $\Gamma^*$  | CO <sub>2</sub> compensation point in absence of 'dark' respiration                              | $\mu\text{mol CO}_2 \text{ mol}^{-1}\text{air}$                                 |
| $R_d$   | Dark respiration rate  | $\mu\text{mol CO}_2 \text{ m}^{-2}_{\text{leaf}} \text{ s}^{-1}$                |
| $K'$  | effective Michaelis-Menten constant for Rubisco  | $\mu\text{mol CO}_2 \text{ mol}^{-1}\text{air}$                                 |
| $K_C$   | Rubisco CO <sub>2</sub> Michaelis-Menten constant  | Pa  |
| $K_O$   | Rubisco O <sub>2</sub> Michaelis-Menten constant   | kPa   |
| $O$   | ambient O <sub>2</sub> partial pressure  | kPa   |
| $\chi_v$  | RuBP carboxylation capacity per unit N   | $\mu\text{mol CO}_2 \text{ s}^{-1} \text{ mmol}^{-1}\text{N}$                   |
| $\chi_j$  | electron transport capacity per unit N   | $\mu\text{mol e}^- \text{ s}^{-1} \text{ mmol}^{-1}\text{N}$                    |
| $k$   | $(\partial A_d / \partial c_i)_{T_i}$ (isothermal slope of the demand curve)                     | $\text{mol air m}^{-2}_{\text{leaf}} \text{ s}^{-1}$                            |
| $\xi$   | $(\partial A_d / \partial T)_{c_i}$  | $\mu\text{mol CO}_2 \text{ m}^{-2}_{\text{leaf}} \text{ s}^{-1} \text{ K}^{-1}$ |
| <i>Parameters specific to the Badeck model of potential electron transport rate</i> |  |   |
| $j$   | potential electron transport rate per unit Chl   | $\mu\text{mol e}^- \text{ s}^{-1} \text{ mmol}^{-1}\text{Chl}$                  |
| $j_m$   | maximum potential electron transport rate per unit Chl   | $\mu\text{mol e}^- \text{ s}^{-1} \text{ mmol}^{-1}\text{Chl}$                  |
| $i_a$   | useful irradiance absorbed by PSII per unit Chl  | $\mu\text{mol photons s}^{-1} \text{ mmol}^{-1}\text{Chl}$                      |
| $i$   | irradiance per unit Chl  | $\text{mmol photons s}^{-1} \text{ mmol}^{-1}\text{Chl}$                        |
| $I^*$   | irradiance below which $J$ is independent of $N$   | $\mu\text{mol photons m}^{-2}_{\text{leaf}} \text{ s}^{-1}$                     |
| $c$   | cumulative Chl content   | $\text{mmol Chl m}^{-2}_{\text{leaf}}$  |
| $c_L$   | total leaf Chl content   | $\text{mmol Chl m}^{-2}_{\text{leaf}}$  |
| $\chi_c$  | Chl per unit N   | $\text{mmol Chl mmol}^{-1}\text{N}$   |
| $k_c$   | light extinction coefficient for Chl   | $[\text{mmol Chl m}^{-2}_{\text{leaf}}]^{-1}$                                   |

**Table 3.** Specific parameter values for simulations that generated the figures. Temperature dependencies (not shown) are those used by de Pury and Farquhar (1997), and values shown are at 25°C.

| Symbol     | Numerical value                  | Units  | Source                      |
|------------|----------------------------------|--|-----------------------------|
| $E_t$      | Various (see figure legends)     | $\text{mmol H}_2\text{O m}^{-2}_{\text{ground}} \text{ s}^{-1}$  | –                           |
| $N_t$      | Various (see figure legends)     | $\text{mmol N m}^{-2}_{\text{ground}}$                           | –                           |
| $\Gamma^*$ | 36.9                             | $\mu\text{mol CO}_2 \text{ mol}^{-1}\text{air}$                  | Caemmerer et al. (1994)     |
| $R_d$      | $0.0089V_m$                      | $\mu\text{mol CO}_2 \text{ m}^{-2}_{\text{leaf}} \text{ s}^{-1}$ | de Pury and Farquhar (1997) |
| $K_C$      | 404                              | $\mu\text{mol CO}_2 \text{ mol}^{-1}\text{air}$                  | Caemmerer et al. (1994)     |
| $K_O$      | 248                              | $\text{mmol O}_2 \text{ mol}^{-1}\text{air}$                     | Caemmerer et al. (1994)     |
| $O$        | 210                              | $\text{mmol O}_2 \text{ mol}^{-1}\text{air}$                     | –                           |
| $\chi_v$   | 1.294                            | $\mu\text{mol CO}_2 \text{ s}^{-1} \text{ mmol}^{-1}\text{N}$    | de Pury and Farquhar (1997) |
| $\chi_j$   | $2.1 \chi_v$                     | $\mu\text{mol e}^- \text{ s}^{-1} \text{ mmol}^{-1}\text{N}$     | de Pury and Farquhar (1997) |
| $\chi_c$   | $4.41610^{-3}$                   | $\text{mmol Chl mmol}^{-1}\text{N}$                              | Badeck (1995)               |
| $F$        | 0.425                            | unitless   | de Pury and Farquhar (1997) |
| $j_m$      | $615.4 (\chi_j / \chi_c)$        | $\mu\text{mol e}^- \text{ s}^{-1} \text{ mmol}^{-1}\text{Chl}$   | Eq A16                      |
| $k_c$      | 5.0                              | $[\text{mmol Chl m}^{-2}_{\text{leaf}}]^{-1}$                    | Badeck (1995)               |
| $I^*$      | $50.9 (\chi_j / [k_c F \chi_c])$ | $\mu\text{mol photons m}^{-2}_{\text{leaf}} \text{ s}^{-1}$      | Eq A17                      |
| $gbh$      | 2.0                              | $\text{mol air m}^{-2}_{\text{leaf}} \text{ s}^{-1}$             | chosen arbitrarily          |
| $c_a$      | 365                              | $\mu\text{mol CO}_2 \text{ mol}^{-1}\text{air}$                  | chosen arbitrarily          |
| $w_a$      | 12                               | $\text{mmol H}_2\text{O mol}^{-1}\text{air}$                     | chosen arbitrarily          |

## A.1 General Gas Exchange Model

### A.1.1 CO<sub>2</sub> Assimilation

To develop analytical expressions for the marginal gains ( $\partial A/\partial E$  and  $\partial A/\partial N$ ; Eqs 5 and 6), we must define the function  $A$  and its derivatives in a precise manner. At steady-state, ignoring diffusive resistance within the leaf, the assimilation rate  $A$  must simultaneously satisfy a ‘supply’ equation ( $A = A_s$ ) describing CO<sub>2</sub> flux from the atmosphere to the site of carboxylation, and a ‘demand’ equation ( $A = A_d$ ) describing the flux of CO<sub>2</sub> that is RuBP carboxylation:

$$A = A_s(g_{tc}, c_a, c_i) = g_{tc}(c_a - c_i) \quad (\text{A1})$$

$$A = A_d(N, I, T_l, c_i) = \minh\{A_V, A_J, \theta_A\} \quad (\text{A2})$$

where  $A_V$  and  $A_J$  are defined by Eqs A8 and A9 below. The hyperbolic minimum function, *minh*, is the negative root of a quadratic expression given by:

$$\minh\{x, y, \theta\} \equiv Z \quad \text{such that} \quad \theta Z^2 - (x + y)Z + xy = 0 \quad (\text{A3})$$

In Eq A3,  $\theta$  is a convexity term, ranging from zero to one, that controls the degree of co-limitation between  $x$  and  $y$  when their values are close. If  $\theta$  is close to unity, there is little colimitation, and the transition between  $x$  and  $y$  is very sharp. In Eq A2  $\theta$  is subscripted with ‘A’ to distinguish it from an analogous term,  $\theta_J$ , in an expression for potential electron transport rate,  $J$ ; see Eq A13.

It is convenient to identify  $c_i$  as a parameter linking CO<sub>2</sub> supply and demand (Eqs A1 and A2), and to express it as a function of all independent variables in the supply and demand equations (removing  $c_a$  as a constant):

$$c_i = c_i(g_{tc}, N, I, T_l) \quad (\text{A4})$$

Total conductance to CO<sub>2</sub> is a function of stomatal and boundary layer components:

$$g_{tc} = (g_{sc}^{-1} + g_{bc}^{-1})^{-1} \quad (\text{A5})$$

Two complete, alternative analytical expressions for assimilation can then be created by nesting this function for  $c_i$  into the supply and demand equations:

$$A = A_s(g_{tc}, c_i(g_{tc}, N, I, T_l)) = g_{tc}(c_a - c_i(g_{tc}, N, I, T_l)) \quad (\text{A6})$$

$$A = A_d(N, I, T_l, c_i(g_{tc}, N, I, T_l)) \quad (\text{A7})$$

In some cases, we will find it more convenient to differentiate Eq A6; in some cases, Eq A7 is more easily analysed. With all dependencies thus contained in a single equation, one can construct mathematical expressions for any partial derivative.

In Eq A2,

$$A_V \equiv \frac{V_m(c_i - \Gamma_*)}{c_i + K'} - R_d, \quad K' \equiv K_C(1 + O/K_O) / P_t \quad (\text{A8})$$

$$A_J \equiv \frac{J(c_i - \Gamma^*)}{4(c_i + 2\Gamma^*)} - R_d \quad (\text{A9})$$

The maximum velocity of RuBP carboxylation,  $V_m$ , is generally taken as a linear and homogeneous function of whole-leaf nitrogen content,  $N$ :

$$V_m = \chi_V N \quad (\text{A10})$$

#### A.1.1.1 Modeling Potential Electron Transport Rate

As described in Section 3, the potential electron transport rate,  $J$ , can be modeled in more than one way. The most common model calculates  $J$  as the lesser of  $J_m$ , the maximum potential electron transport rate, and  $I_a$ , the useful irradiance absorbed by Photosystem II. Importantly,  $J_m$  and  $I_a$  are calculated from whole-leaf parameters:  $J_m$  is assumed linearly proportional to whole-leaf N content,  $N$ , and  $I_a$  is the product of incident irradiance,  $I$ , with absorptance,  $\alpha$ , and a spectral correction factor,  $F$ :

$$J_m = \chi_j N \quad (\text{A11})$$

$$I_a = \alpha FI \quad (\text{A12})$$

$$J = \min\{J_m, I_a, \theta_J\} = \min\{\chi_j N, \alpha FI, \theta_J\} \quad (\text{A13})$$

However, the leaf absorptance,  $\alpha$ , is determined by leaf chlorophyll content,  $c_L$ , which is also limited by nitrogen. Badeck (1995) developed an alternative model that calculates  $J$  by integrating the local potential electron transport rate per unit of chlorophyll,  $j$ , over all 'layers' of chlorophyll. The layers are ordinated by cumulative chlorophyll density,  $c$ , so that the value of  $c$  in the 'lowest' layer is  $c_L$  (which Badeck assumed is proportional to whole-leaf  $N$  by a constant:  $c_L = \chi_c N$ ). Chlorophyll is assumed to absorb irradiance in proportion to its local intensity, so the useful irradiance absorbed by PSII declines exponentially with  $c$  with an extinction coefficient  $k_c$ :

$$di(c)/dc = -k_c i(c) \Rightarrow i(c) = i(0)e^{-k_c c} = k_c I e^{-k_c c}, \quad i_a(c) = Fi(c) \quad (\text{A14})$$

Note that the leaf absorptance can easily be calculated from Eq A14 as

$$\alpha = \frac{i(0) - i(c_L)}{i(0)} = 1 - e^{-k_c c_L} \quad (\text{A15})$$

However, Badeck also assumed that the amount of nitrogen allocated to electron transport per unit of chlorophyll, and therefore also  $j_m$ , the maximum potential electron transport rate per unit of chlorophyll, is the same for all layers (and it can easily be shown that  $j_m = \chi_j/\chi_c$ ). As a result, in any given layer,  $j$  can be limited either by nitrogen or by light:

$$j(c) = \min\{j_m, i_a(c)\} = \min\left\{\frac{\chi_j}{\chi_c}, k_c F I e^{-k_c c}\right\} \quad (\text{A16})$$

Whole-leaf  $J$  is calculated by integrating  $j(c)$  from  $c = 0$  to  $c = c_L$ . The result has three different cases (Fig. 5; Eq A17): either (a) all layers are nitrogen-limited, (b) some layers are light-limited and some are nitrogen-limited, or (c) all layers are light-limited.

Mathematically,

$$J = \begin{cases} J_m & (a) I \geq I^* e^{k_c \chi_c N} \\ J_m \ln(I/I^*) + I_a \left( \frac{I^*/I - e^{-k_c \chi_c N}}{1 - e^{-k_c \chi_c N}} \right) & (b) I^* < I < I^* e^{k_c \chi_c N} \\ I_a & (c) I \leq I^* \end{cases} \quad \text{where } I^* \equiv \frac{\chi_j}{k_c F \chi_c} \quad (A17)$$

where  $J_m$  and  $I_a$  are defined by Eqs A11 and A12, with leaf absorbance  $\alpha$  given by Eq A15. The term  $I^*$  is the incident irradiance at which the light- and nitrogen-limitations are exactly balanced in the uppermost layer (i.e.,  $j_m = i_a(0)$ ).  $I^*$  is proportional to the whole-leaf electron transport capacity per unit of chlorophyll, which, in Badeck's model, is constant and therefore independent of leaf N content. If the actual irradiance,  $I$ , is large enough to saturate the electron transport capacity of the lowest layer, then all layers are nitrogen-limited and  $J = J_m$  (Fig. 5a; part (a) in Eq A17). Conversely, if  $I$  is lower than  $I^*$ , then all layers are light-limited (Fig. 5c; part (c) in Eq A17). For intermediate values of  $I$ , a transition from N- to light-limitation occurs within the leaf (Fig. 5b; part (b) in Eq A17).

### A.1.2 Transpiration and Energy Balance

Transpiration ( $E$ ) is the product of total conductance,  $g_{tw}$ , and the gradient of water vapor mole fraction from the intercellular spaces ( $w_i$ ) to the ambient air ( $w_a$ ):

$$E = E(g_{tw}, w_i(T_l), w_a) = g_{tw}(w_i(T_l) - w_a) \quad (A18)$$

Transpiration and assimilation are linked by stomatal conductance (which is to be optimized, and is thus unconstrained) and by energy balance, which constrains  $T_l$ . We present an energy balance expression, which is an implicit function for  $T_l$ , because we will need to differentiate it to account for thermal effects on  $\partial A/\partial E$  in the next section:

$$\Phi = f_L \sigma (T_l^4 - \varepsilon_{atm} T_a^4) + l \cdot E + c_{pa} g_{bh} (T_l - T_a) \quad (A19)$$

In Eq A19,  $\Phi$  is absorbed solar radiation,  $T_a$  is air temperature,  $\sigma$  is the Stefan-Boltzmann constant ( $5.67 \cdot 10^{-8} \text{ J m}^{-2} \text{ K}^{-4} \text{ s}^{-1}$ ),  $\varepsilon_{atm}$  is the atmospheric transmissivity,  $l$  is the latent heat of vaporization ( $18.01 \text{ J mol}^{-1} \text{ H}_2\text{O}$  at  $25^\circ\text{C}$ ), and  $c_{pa}$  is the heat capacity of air ( $29.25 \text{ J mol}^{-1} \text{ air K}^{-1}$  at  $25^\circ\text{C}$ ). The term  $f_L$  decreases with depth in the canopy (i.e., with increasing  $L$ ), because lower leaves are less radiatively coupled to the sky. Both  $f_L$  and  $\Phi$  are calculated from the detailed canopy light penetration model, and formal expressions for  $\Phi$  and  $f_L$ , and also for  $\varepsilon_{atm}$  and  $g_{bh}$ , can be found in Leuning et al. (1995) and de Pury and Farquhar (1997).

### A.2 Derivation of an Expression for $\partial A/\partial E$ at Constant N

Eq 5 says that a plant is making optimal use of a finite, fixed water supply if the marginal gain of assimilation rate with respect to transpiration rate is uniform and constant. We proceed below to identify a formula for this marginal gain:

$$\left( \frac{\partial A}{\partial E} \right)_{N,env} \equiv \frac{dA_\lambda}{dE} = \frac{(dA_\lambda/dg_{tw})}{(dE/dg_{tw})} = \omega \frac{(dA_\lambda/dg_{tc})}{(dE/dg_{tw})} \quad (A20)$$

In Eq A20, the partial derivative at constant  $N$  and constant environmental conditions has been rewritten as a total derivative for clarity in the ensuing derivation; in essence, we have redefined Eqs A6 and A7 as follows:

$$A_\lambda \equiv A_{s\lambda}(g_{tc}, c_i(g_{tc}, T_l)) \quad (\text{A21})$$

$$A_\lambda \equiv A_{d\lambda}(T_l, c_i(g_{tc}, T_l)) \quad (\text{A22})$$

The transpiration rate does not depend on  $N$  explicitly, so it is not necessary to redefine  $E$  for this derivation. The term  $\omega$  relates the differentials of  $g_{tc}$  and  $g_{tw}$ , accounting for the ratio of  $\text{H}_2\text{O}$  and  $\text{CO}_2$  diffusivities through stomata (1.6):

$$\omega \equiv \frac{dg_{tc}}{dg_{tw}} = \frac{dg_{tc}/dg_{sc}}{dg_{tw}/dg_{sw}} \cdot \frac{dg_{sc}}{dg_{sw}} = \frac{(g_{tc}/g_{sc})^2}{1.6 \cdot (g_{tw}/g_{sw})^2} = 1.6 \cdot \frac{g_{tc}^2}{g_{tw}^2} \quad (\text{A23})$$

To evaluate the derivative of  $A_\lambda$  with respect to  $g_{tc}$ , we choose the ‘demand’ equation for assimilation, Eq A7:

$$\frac{dA_\lambda}{dg_{tc}} = \frac{dA_{d\lambda}}{dg_{tc}} = \left( \frac{\partial A_{d\lambda}}{\partial c_i} \right)_{T_l} \frac{dc_i}{dg_{tc}} + \left( \frac{\partial A_{d\lambda}}{\partial T_l} \right)_{c_i} \frac{dT_l}{dg_{tc}} \quad (\text{A24})$$

The partial derivatives in Eq A24 are given by:

$$\left( \frac{\partial A_{d\lambda}}{\partial c_i} \right)_{T_l} \equiv k = \left\{ \begin{array}{ll} \frac{V_m(K' + \Gamma_*)}{(c_i + K')^2} & \text{if } A_V < A_J, \\ \frac{3J\Gamma_*}{4(c_i + 2\Gamma_*)^2} & \text{if } A_J < A_V \end{array} \right\} \quad (\text{A25})$$

$$\left( \frac{\partial A_{d\lambda}}{\partial T_l} \right)_{c_i} = \sum^i \left( \frac{\partial A_{d\lambda}}{\partial X_i} \right)_{c_i} \left( \frac{dX_i}{dT_l} \right) \equiv \xi \quad (\text{A26})$$

In Eq A26 the  $X_i$  are elements of a vector,  $\mathbf{X}$ , containing temperature-sensitive photosynthetic parameters:  $\mathbf{X} = \{V_m, J, K_c, K_o, \Gamma_*, R_d\}$ . The simulations presented in this study used the temperature dependencies given by de Pury and Farquhar (1997), which are not reproduced here. Note that implementation of Eqs A25 and A26 in a computer program requires caution, because the code must choose the functions corresponding to the locally limiting phase of the biochemical model. Importantly, if the transition between the two phases of the photosynthesis model is ‘smoothed’ hyperbolically as in Eq A2, then Eqs A25 and A26 are not strictly correct. Instead, Eq A3, which is a composite function of the two phases,  $A_V$  and  $A_J$ , must be differentiated, and then the separate derivatives of  $A_V$  and  $A_J$  must be substituted into the result. From Eq A3, the general expression for a derivative of the hyperbolic minimum of two functions is:

$$Z' = \frac{x'(Z - y) + y'(Z - x)}{(\theta Z - y) + (\theta Z - x)} \quad (\text{A27})$$

where  $x$  and  $y$  are the two functions and  $Z$  is their smoothed minimum. The primes in Eq A27 represent differentiation. Applied to Eq A25,  $Z'$  represents  $k$ ,  $x$  and  $y$  represent  $A_V$  and  $A_J$ , and  $x'$  and  $y'$  represent  $\partial A_V/\partial c_i$  and  $\partial A_J/\partial c_i$  (the two expressions on the right-hand side of Eq A25), respectively.

Eq A24 also contains total derivatives of  $c_i$  and  $T_l$  with respect to  $g_{tc}$ , which require some minor algebraic acrobatics to solve. To find  $dc_i/dg_{tc}$ , we will find the total derivative of the ‘supply’ version of  $A_\lambda$  with respect to  $g_{tc}$ , set it equal to the derivative of the ‘demand’

version of  $A_\lambda$  (recognizing that these two are equal when CO<sub>2</sub> diffusion is at steady state), and solving the result for the derivative of  $c_i$  with respect to  $g_{tc}$ .

$$\frac{dA_\lambda}{dg_{tc}} = \frac{dA_{s\lambda}}{dg_{tc}} = \left( \frac{\partial A_{s\lambda}}{\partial g_{tc}} \right)_{c_i} + \left( \frac{\partial A_{s\lambda}}{\partial c_i} \right)_{g_{tc}} \frac{dc_i}{dg_{tc}} \tag{A28}$$

$$\frac{dA_{s\lambda}}{dg_{tc}} = \frac{dA_{d\lambda}}{dg_{tc}} \Rightarrow \frac{dc_i}{dg_{tc}} = \frac{\left( \frac{\partial A_{s\lambda}}{\partial g_{tc}} \right)_{c_i} - \left( \frac{\partial A_{d\lambda}}{\partial T_l} \right)_{c_i} \frac{dT_l}{dg_{tc}}}{\left( \frac{\partial A_{d\lambda}}{\partial c_i} \right)_{T_l} - \left( \frac{\partial A_{s\lambda}}{\partial c_i} \right)_{g_{tc}}} \tag{A29}$$

Eq A29 contains four partial derivatives. The two derivatives of  $A_d$  are given in Eqs A25 and A26; those for  $A_s$  are easily found from Eq A6:

$$\left( \frac{\partial A_{s\lambda}}{\partial g_{tc}} \right)_{c_i} = (c_a - c_i) \equiv \Delta c \tag{A30}$$

$$\left( \frac{\partial A_{s\lambda}}{\partial c_i} \right)_{g_{tc}} = -g_{tc} \tag{A31}$$

To find the remaining term ( $dT_l/dg_{tc}$ ) in Eq A29, we differentiate the heat balance expression (Eq A19) with respect to  $g_{tc}$  and solve:

$$0 = f_L \sigma \left( 4T_l^3 \frac{dT_l}{dg_{tc}} \right) + l \frac{dE}{dg_{tc}} + c_{pa} g_{bh} \frac{dT_l}{dg_{tc}} \tag{A32}$$

$$\frac{dT_l}{dg_{tc}} = \frac{-l(dE/dg_{tc})}{4f_L \sigma T_l^3 + c_{pa} g_{bh}} \tag{A33}$$

The derivative of  $E$  with respect to  $g_{tc}$  is easily obtained from Eq A18:

$$\frac{dE}{dg_{tc}} = \omega \frac{dE}{dg_{tw}} = \omega \left[ \left( \frac{\partial E}{\partial g_{tw}} \right)_{w_i} + \left( \frac{\partial E}{\partial w_l} \right)_{g_{tw}} \frac{dw_l}{dg_{tw}} \right] \tag{A34}$$

where

$$\left( \frac{\partial E}{\partial g_{tw}} \right)_{w_i} = w_i - w_a \equiv \Delta w \tag{A35}$$

$$\left( \frac{\partial E}{\partial w_l} \right)_{g_{tw}} = g_{tw} \tag{A36}$$

$$\frac{dw_l}{dg_{tw}} = \frac{dw_l}{dT_l} \frac{dT_l}{dg_{tc}} \frac{1}{\omega} \tag{A37}$$

Substituting Eqs A35–A37 back into Eq A34, we have

$$\frac{dE}{dg_{tc}} = \omega \Delta w + s g_{tw} \frac{dT_l}{dg_{tc}} \tag{A38}$$

The dependence of saturation vapor pressure on temperature (in Eq A37, the derivative of  $w_l$  with respect to  $T_l$ ) has been replaced in Eq A38 by  $s$ , its conventional symbol;  $s$  is an exponential function of  $T_l$ . Eqs A22 and A38 are combined and rearranged to yield an expression for  $dT_l/dg_{tc}$ :

$$\frac{dT_l}{dg_{tc}} = \omega \cdot \frac{dT_l}{dg_{tw}} = \omega \cdot \frac{-l \Delta w}{l s + c_{pa} g_{bh} + 4 f_L \sigma T_l^3} \equiv \omega \cdot T_l' \quad (\text{A39})$$

All of the pieces are now in place to complete the expression (Eq A20) for  $dA_\lambda/dE$ :

$$\frac{dA_\lambda}{dE} = \left( \frac{\Delta c + g_{tc} [\xi T_l'] / [k \omega]}{\Delta w + g_{tw} [s T_l']} \right) \cdot \left( \frac{k}{k + g_{tc}} \right) \cdot \omega \stackrel{opt}{=} \frac{1}{\lambda} \quad (\text{A40})$$

The first term can be identified as the ratio of the driving gradients for photosynthesis and transpiration, with conductance-weighted temperature effects (in brackets); The second term expresses the relative biochemical limitation to photosynthesis, because it moves between unity and zero as stomatal conductance varies from zero to infinity. The third term ( $\omega$ ) balances the conductances to water and  $\text{CO}_2$ , and accounts for the different effects of boundary layer conductance on  $E$  and  $A$ .

Eq A38 can be simplified into the following form, replacing  $g_{tc}$  with  $g$  for clarity:

$$\frac{1}{\lambda} = \left( \frac{k}{k + g} \right) \cdot \frac{1}{\hat{\lambda}} \quad (\text{A41})$$

The last term,  $\hat{\lambda}$ , is the limiting, minimum value that  $\lambda$  would approach if the slope of the demand curve,  $k$ , approached infinity. The meanings of  $\hat{\lambda}$  (and its counterpart for nitrogen,  $\hat{v}$ , defined by Eqs A50 and A54 below) are clarified by Fig. 7.  $\hat{\lambda}$  may be thought of as the lowest possible cost of carbon in units of water (measured at a given  $c_i$ ). The actual cost,  $\lambda$ , is larger because, when an increase in conductance provides more  $\text{CO}_2$ , some of that carbon never gets fixed – instead, it stays in the intercellular spaces (where it increases  $c_i$ ), because the photosynthetic apparatus has finite efficiency.

### A.3 Derivation of an Expression for $\partial A/\partial N$ at Constant E

Optimal nitrogen use is achieved when the sensitivity of assimilation to leaf nitrogen is uniform throughout the canopy. It is not possible for this sensitivity to be constant in time, because nitrogen can not be moved among leaves with anywhere near the speed that would be required to track diurnal changes in irradiance. Therefore, the gain function in this case is actually the daily integral, or the time-average over one day, of assimilation:

$$\bar{A} \equiv \int_{day} A(t, L) dt \Big/ \int_{day} dt \quad (\text{A42})$$

We require a formula for the response of daily-averaged  $A$  to leaf N content,  $N$ , at constant transpiration rate,  $E$ . When this derivative is invariant, we symbolize its numerical value by  $1/v$ .

$$\left( \frac{\partial \bar{A}}{\partial N} \right)_{E, env} \equiv \frac{d\bar{A}_v}{dN} = \frac{1}{t_{dl}} \frac{d}{dN} \int_{day} A_v(t, L) dt = \frac{1}{t_{dl}} \int_{day} \frac{dA_v}{dN}(t) dt \stackrel{opt}{=} \frac{1}{v} \quad (\text{A43})$$

Pulling the differential operator  $d/dN$  into the integral is permitted because the domain of differentiation is orthogonal to the domain of integration (i.e.,  $dN/dt$  is zero). This simplifies

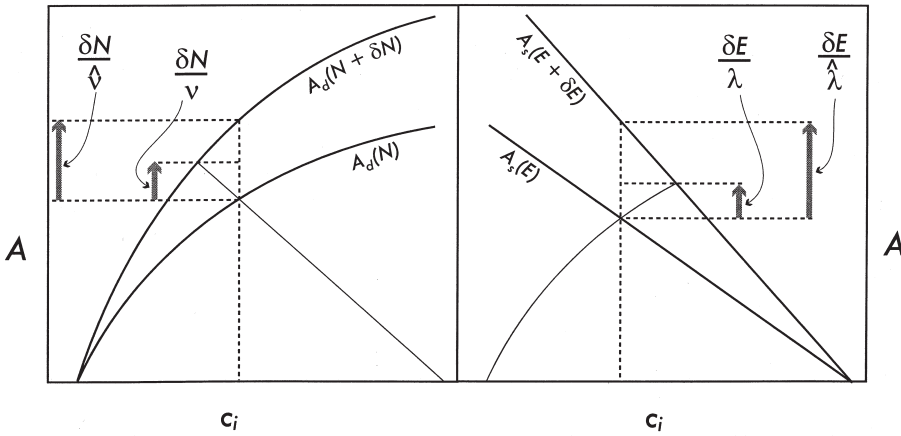


**Fig. 7.** Diagram representing the meanings of (a)  $\hat{v}$  ( $\equiv (\partial A/\partial N)_{T_l, c_i}$ , Eqs A50 and A54) and (b)  $\hat{\lambda}$  ( $\equiv (\partial A/\partial E)_{T_l, c_i}$ , Eqs A40 and A41), the isothermal sensitivities of assimilation rate to leaf N content and transpiration rate, respectively, at constant  $c_i$ . In the left panel, a demand curve ( $A_d$ ) is shown before and after an incremental change ( $\delta N$ ) in leaf nitrogen content ( $N$ ).  $\delta N/v$  (where  $v$  is the sensitivity of  $A$  to  $N$  at constant  $E$ , rather than at constant  $c_i$ ; Eq A54) is the gain in assimilation that would be realized if no change occurred in the supply curve (shown as a fainter straight line), that is, if stomatal conductance did not change with leaf  $N$ .  $\delta N/\hat{v}$  is the ‘potential’ gain – the gain that would be realized if the supply curve’s finite slope did not cause  $c_i$  to decrease as  $N$  increased. Similarly, in (b), supply curves are shown before and after an increment in  $E$ , and the corresponding gain and potential gain (the latter not limited by the demand curve’s finite slope) are  $\delta E/\lambda$  and  $\delta E/\hat{\lambda}$ , respectively.

the problem somewhat, in that we can find the ‘local’ derivative  $dA/dN$  for analytical purposes, and integrate it only for computational or graphical implementation. We begin by redefining the assimilation functions appropriate to the domain of optimization. In this case,  $dA/dN$  compares among candidate values of  $N$  at one depth (more precisely, one value of cumulative leaf area index,  $L$ ) in the individual plant canopy, and the timecourse of stomatal conductance is invariant among candidate  $N$  values:

$$A_v = A_{sv}(c_i(T_l, N)) \tag{A44}$$

$$A_v = A_{dv}(N, T_l, c_i(T_l, N)) \tag{A45}$$

Differentiating the supply and demand functions, recognizing that leaf temperature has no explicit dependence on  $N$ , and setting the results equal, we have the following:

$$\frac{dA_v}{dN} = \frac{dA_{sv}}{dN} = \frac{dA_{dv}}{dN} \tag{A46}$$

$$\frac{dA_{sv}}{dN} = -g_{tc} \frac{dc_i}{dN} \tag{A47}$$

$$\frac{dA_{dv}}{dN} = \left( \frac{\partial A_{dv}}{\partial N} \right)_{T_l, c_i} + k \frac{dc_i}{dN} \tag{A48}$$

Solving these for  $dc_i/dN$  and substituting the result into the second part of the preceding equation, we have

$$\frac{dA_v}{dN} = \left( \frac{g_{tc}}{g_{tc} + k} \right) \left( \frac{\partial A_{dv}}{\partial N} \right)_{T_i, c_i} \quad (\text{A49})$$

where

$$\left( \frac{\partial A_d}{\partial N} \right)_{T_i, c_i} = (A + R_d) \frac{d \ln W}{dN} - \frac{R_d}{N}, \quad W = \begin{cases} V & \text{if } A = A_v \\ J & \text{if } A = A_j \end{cases} \quad (\text{A50})$$

The relative responses of  $V$  and  $J$  to  $N$  ( $d \ln W/dN$  in Eq A50) can be calculated from Eqs A10–A17. From Eq A10,  $d \ln V/dN$  is simply  $1/N$ . However,  $d \ln J/dN$  is different for the superleaf (Eqs A11–A13) and Badeck (Eqs A14–A17) models of potential electron transport rate. For the superleaf model,  $d \ln J/dN$  is calculated by differentiating the hyperbolic minimization function (Eq A3) with respect to  $N$ , solving for  $dJ/dN$ , and dividing by  $J$ :

$$\frac{d \ln J}{dN} = \frac{\chi_j}{J} \left( \frac{J - I_a}{2\theta J - J_m - I_a} \right) \quad (\text{A51})$$

For the Badeck model, the corresponding expressions are very simple when the leaf is either entirely N-limited or entirely light-limited, but the result is quite complex at intermediate irradiances:

$$\frac{d \ln J}{dN} = \begin{cases} \frac{1/N}{\alpha \chi_j \ln(I/I^*) + k_c \chi_c I_a (1 - \alpha)} & (a) \quad I \geq I^* e^{k_c \chi_c N} \\ \frac{1/N}{\alpha J_m \ln(I/I^*) + I_a (I/I^* - 1 + \alpha)} & (b) \quad I^* < I < I^* e^{k_c \chi_c N} \\ \frac{1/N}{k_c \chi_c (1 - \alpha)} & (c) \quad I \leq I^* \end{cases} \quad (\text{A52})$$

(The terms  $I^*$  and  $\alpha$  in Eq A52 are defined in Eqs A15 and A17.) As discussed in the text, invariance of  $dA/dN$  on short time scales is not generally possible, so the optimal criterion is actually invariance in the derivative of  $A$  averaged over a day. Because  $N$  is constant within a day, the derivative can enter the integral:

$$\frac{d\bar{A}_v}{dN} = \int_{\text{day}} \left( \frac{g_{tc}}{g_{tc} + k} \right) \left( \frac{\partial A_{dv}}{\partial N} \right)_{T_i, c_i} dt \Big/ \int_{\text{day}} dt \stackrel{\text{opt}}{\equiv} \frac{1}{v} \quad (\text{A53})$$

The quantity  $1/v$  clearly increases in a saturating fashion as the water limitation diminishes (that is, as conductance increases). The partial derivative on the right side of Eq A53 thus represents an extreme value of  $1/v$  wherein water is not at all limiting ( $g_{tc} \rightarrow \infty$ ) – i.e., it is the value of  $dA/dN$  that would obtain if  $g_{tc}$  could increase arbitrarily to match any increase in photosynthetic demand, thereby keeping  $c_i$  constant. We denote this limiting value by  $\hat{v}$ , and as before, replace  $g_{tc}$  with  $g$  for clarity.  $\hat{v}$  is explained graphically by Fig. 7.

$$\frac{1}{v} = \int_{\text{day}} \left( \frac{g}{g + k} \right) \cdot \frac{1}{\hat{v}} dt \Big/ \int_{\text{day}} dt \quad (\text{A54})$$

### A.4 Derivation of an Expression for $\partial A/\partial N$ for Varying E

When water and nitrogen use are optimized at the same time, invariance of  $v$  specifies the optimal N distribution (Section 2.3). However, there may be some situations when one could not assume, or would not wish to assume that water use is optimal, and yet one would nevertheless wish to identify optimal nitrogen distributions. For example, one may wish to evaluate the relative efficiency of nitrogen distributions in a canopy model in which stomatal conductance is predicted by an empirical submodel. In such cases, it is necessary to apply the general criterion for optimal nitrogen use (invariance of  $\eta$  among canopy layers; Eq 8) rather than the criterion that applies when water use is also optimal (invariance of  $v$ ; Eq 14). The relevant derivative (Eq 8) is:

$$\left(\frac{\partial \bar{A}}{\partial N}\right)_{env} \equiv \frac{d\bar{A}_\eta}{dN} = \frac{1}{t_{dl}} \frac{d}{dN} \int_{day} A_\eta(t, L) dt = \frac{1}{t_{dl}} \int_{day} \frac{dA_\eta}{dN}(t) dt \equiv \frac{1}{\eta} \tag{A55}$$

As in the derivation of  $v$ , we redefine the gain function relative to the domain of optimisation, which in this case must allow stomatal conductance to vary arbitrarily:

$$A_\eta = A_{s\eta}(g_{tc}, c_i(g_{tc}, T_l, N)) \tag{A56}$$

$$A_\eta = A_{d\eta}(N, T_l, c_i(g_{tc}, T_l, N)) \tag{A57}$$

We differentiate the supply and demand equations, then set the results equal and solve for  $dc_i/dN$ :

$$\frac{dA_\eta}{dN} = \frac{dA_{s\eta}}{dN} = \left(\frac{\partial A_{s\eta}}{\partial g_{tc}}\right)_{c_i} \frac{dg_{tc}}{dN} + \left(\frac{\partial A_{s\eta}}{\partial c_i}\right)_{g_{tc}} \frac{dc_i}{dN} = \Delta c \frac{dg_{tc}}{dN} - g_{tc} \frac{dc_i}{dN} \tag{A58}$$

$$\frac{dA_\eta}{dN} = \frac{dA_{d\eta}}{dN} = \left(\frac{\partial A_{d\eta}}{\partial N}\right)_{T_l, c_i} + \left(\frac{\partial A_{d\eta}}{\partial T_l}\right)_{T_l, c_i} \frac{dT_l}{dN} + \left(\frac{\partial A_{d\eta}}{\partial c_i}\right)_{T_l, N} \frac{dc_i}{dN} = \frac{1}{\hat{v}} + \xi \frac{dT_l}{dN} + k \frac{dc_i}{dN} \tag{A59}$$

$$\frac{dA_\eta}{dN} = \left(\frac{g_{tc}}{g_{tc} + k}\right) \cdot \left[ \left(\frac{\partial A_{d\eta}}{\partial N}\right)_{T_l, c_i} + \frac{dg_{tc}}{dN} \cdot \left(\xi \frac{dT_l}{dg_{tc}} - k \frac{\Delta c}{g_{tc}}\right) \right] \tag{A60}$$

This expression separates the response of photosynthesis to nitrogen into two components. One component – the first term in the brackets in Eq A60, and its multiplier to the left of the brackets – represents what may be abstractly considered ‘first-order’ linkage between water and nitrogen optimization. The second term in the square brackets above contains a second-order effect of stomatal conductance in  $dg_{tc}/dN$ . This term represents the fact that stomata may ‘respond’ in some sense to a change in photosynthetic capacity via  $N$ . However, that response is arbitrary and therefore impossible to describe by a consistent mathematical formula, unless stomatal behavior is constrained in some fashion (for example, by an empirical model that includes a stomatal response of  $g_{tc}$  to  $N$ ). If conductance is constrained by optimal water use, an expression for  $dg_{tc}/dN$  could be obtained by differentiating  $\lambda$  with respect to  $N$  and setting the result equal to zero (because  $\partial A/\partial E|_N$  is constant, at  $1/\lambda$ ). Ironically, however, the assumption of constant  $\lambda$  obviates the need to develop  $dg_{tc}/dN$ : in that case, the criterion of optimal nitrogen use degenerates from invariance of  $\eta$  to invariance of  $v$ , and the latter lacks any second-order linkage between  $g_{tc}$  and  $N$ .

### A.5 Numerical Solution Techniques Used to Generate Figs. 2, 4 and 6

Optimal canopy nitrogen profiles were inferred using the model described above, in conjunction with a canopy light penetration model (de Pury and Farquhar 1997) and a simple model of intra-canopy aerodynamics (Leuning et al. 1995), as follows. The canopy was discretised in space, with layers  $0.05 \text{ m}^2_{\text{leaf}} \text{ m}^{-2}_{\text{ground}}$  thick (evaluated in the middle of each layer, i.e., at  $L = 0.025, 0.075$  and so forth), and in time, with timesteps equal to one twelfth of the daylength. The daylength, which depends on geographic location and time of year, was calculated from equations presented by de Pury and Farquhar (1997). Linear summation was used to integrate all relevant variables (the values of each variable at each point were summed, multiplied by the ratio of the stepsize to the total domain).

The optimal values of  $g_{sc}$  and  $N$  were calculated by a nested iterative solution procedure, as follows. (a) Appropriate values of  $\lambda$  and  $\eta$  were arbitrarily chosen. (b) For one canopy layer (one value of  $L$ ), a ‘candidate’ value of leaf N content ( $N$ ) was posited. (c) For one timestep within this layer (one value of  $t$ ), a candidate value of stomatal conductance ( $g_{sc}$ ) was posited, and leaf temperature ( $T_l$ ) was determined by iterative solution of energy balance (Eq A19) using values for incoming radiation, boundary layer conductance, and air temperature calculated from the radiation and aerodynamics submodels of de Pury and Farquhar (1997) and Leuning et al. (1995) ( $T_l$  was adjusted until the ratio of the right- and left-hand sides of Eq A19 was within  $10^{-6}$  of unity). (d)  $(\partial A/\partial E)_N$  was calculated for these values of  $t, L, N$ , and  $g_{sc}$ , and  $T_l$ , using Eq A40. (e) Steps (c) and (d) were repeated for different values of  $g_{sc}$  until the ratio of  $(\partial A/\partial E)_N$  and the chosen ‘target’ value of  $1/\lambda$  was within  $10^{-5}$  of unity. (f) Steps (c) through (e) were repeated for each timestep within the layer, and the daily mean assimilation rate was calculated. (g) Step (f) was repeated for a slightly larger value of leaf N content ( $N(1+10^{-10})$ ) to estimate  $\partial A/\partial N$  numerically. (h) Steps (c) through (g) were repeated for different values of  $N$  until the ratio of  $\partial A/\partial N$  and the chosen target value of  $1/\eta$  was within  $10^{-2.5}$  of unity. (i) Steps (b) through (h) were repeated for all canopy layers, and the resulting canopy totals for assimilation, transpiration, and nitrogen content ( $A_t, E_t$  and  $N_t$ , respectively) were calculated by linear integration.

Numerical values of  $\lambda, \eta$  and  $L_t$  that yielded pairs of canopy profiles with nearly identical values of  $E_t$  and  $N_t$  from two different versions of the model (e.g., superleaf- or Badeck-based models, as for Fig. 4; see the legends for Figs. 2, 4 and 6 for details) were identified as follows: (j) The entire procedure described in the preceding paragraph was repeated for many values of  $\lambda$  and  $\eta$  for each of the two model versions being compared. (k) For each ‘canopy’ thus generated,  $N_t$  and  $E_t$  were plotted against each other (with  $L_t$  being the implicit variable). (l) Many pairs of  $N_t$  vs  $E_t$  curves (one for each of the two model versions being compared) were overlaid until an intersection point was found. At this intersection, the two model versions produced canopies with nearly identical values for both  $E_t$  and  $N_t$  (generally with different values of  $L_t$  for each model version), allowing the two model versions to be compared for the same resource constraints.